AWARD NUMBER: W81XWH-13-1-0147

TITLE: Bisphosphonates in the prevention of post-traumatic osteoarthritis.

PRINCIPAL INVESTIGATOR: Christopher Price (Partnering PI)

CONTRACTING ORGANIZATION: University of Delaware
Newark, DE 19716-0099

REPORT DATE: July 2016

TYPE OF REPORT: Annual

PREPARED FOR: U.S. Army Medical Research and Materiel Command
Fort Detrick, Maryland 21702-5012

REPORT DOCUMENTATION PAGE

Form Approved
OMB No. 0704-0188

1. REPORT DATE	2. REPORT TYPE	3. DATES COVERED
July 2016	Annual	1Jul2015 - 30June2016

4. TITLE AND SUBTITLE
Bisphosphonates in the prevention of post-traumatic osteoarthritis.

5a. CONTRACT NUMBER

5b. GRANT NUMBER
W81XWH-13-1-0147

5c. PROGRAM ELEMENT NUMBER

6. AUTHOR(S)
Christopher Price

E-Mail: cprice@udel.edu

5d. PROJECT NUMBER

5e. TASK NUMBER

5f. WORK UNIT NUMBER

7. PERFORMING ORGANIZATION NAME(S) AND ADDRESS(ES)
University of Delaware
220 Hullihen Hall
Newark DE 19716-0099

8. PERFORMING ORGANIZATION REPORT NUMBER

9. SPONSORING / MONITORING AGENCY NAME(S) AND ADDRESS(ES)

U.S. Army Medical Research and Materiel Command
Fort Detrick, Maryland 21702-5012

10. SPONSOR/MONITOR'S ACRONYM(S)

11. SPONSOR/MONITOR'S REPORT NUMBER(S)

12. DISTRIBUTION / AVAILABILITY STATEMENT

Approved for Public Release; Distribution Unlimited

13. SUPPLEMENTARY NOTES

14. ABSTRACT

The following accomplishments with regard to the Aim 2 tasks (partnering-PI C. Price's responsibility) for grant PR120788P1 during the reporting period from 08/01/2015 to 07/30/2016 are noted.

The animal surgery model (DMM) and drug-delivery methodology (intra-articular injection), which constitute the majority of the proposed research in Aim 2 have completed. The entire cohorts of the Baseline, Age-Matched, SHAM controls, DMM Surgery and DMM + i.a. zoledronic acid (ZA) groups have been collected and analyzed by histology and u-CT analysis. Through the study of this pre-clinical mouse injury model we have established that changes in joint health, including cartilage composition and structure, and joint morphology appear very quickly following injury and are driven by very focal changes in chondrocyte health. In our animal model these changes are seen as early as 3-days post-injury and it is not unreasonable to assume that similar early changes are occurring clinically in human patient that have experienced traumatic joint injury. We have also demonstrated that while a single i.a. injection of ZA post-injury does not provide anti-osteoarthritic benefits in the mouse DMM-model of PTOA, multiple injections (4) over the course of 21-days does provide a degree of protection against cartilage damage. These findings establish a framework to investigate the *in vivo* mechanisms underlying the efficacy of i.a. ZA in treating PTOA, and demonstrate the promise that i.a. ZA holds for the clinical translation of i.a. ZA in treating PTOA following joint injury.

15. SUBJECT TERMS
Post-traumatic osteoarthritis; cartilage degeneration; DMM model; bisphosphonate; zoledronic acid; chondro-protection; cartilage therapy

16. SECURITY CLASSIFICATION OF: U			17. LIMITATION OF ABSTRACT	18. NUMBER OF PAGES	19a. NAME OF RESPONSIBLE PERSON
a. REPORT	b. ABSTRACT	c. THIS PAGE			USAMRMC
Unclassified	Unclassified	Unclassified	Unclassified	67	19b. TELEPHONE NUMBER *(include area code)*

Table of Contents

1. **INTRODUCTION:** This grant focuses on the investigation of a pharmacological treatment for "post-traumatic osteoarthritis" (PTOA). PTOA is a disease of cartilage degeneration that results from acute joint trauma (*e.g.,* torn cartilage, dislocated joints, and meniscal or ligamentous damage) (*1*, *2*), injuries that are common in military service (*3*, *4*). Currently, no preventative or curative treatments exist for PTOA, and afflicted individuals are resigned to the gradual degeneration and loss-of-function of the joint with few therapeutic options other than costly and highly invasive late-stage surgical approaches, including micro-fracture surgery and joint replacement. In a proof-of-concept study we reported that repeated systemic administration of the FDA-approved bisphosphonate drug zoledronic acid (ZA) immediately following joint injury could suppress the development of PTOA in the DMM (destabilization of the medial meniscus) mouse model of PTOA (*5*). However, the strong, and potential deleterious impact of BPs on bone remodeling (*6*, *7*) and their resultant side effects represents a barrier to their systemic use in the clinical treatment of PTOA. In this grant, we proposed and are testing the efficacy of targeted ZA delivery, through localized intra-articular (i.a.) injection, to prevent PTOA while minimizing adverse skeletal health effects. Furthermore, we are exploring the cellular and molecular mechanisms underlying ZA's anti-osteoarthritic potential in order to develop therapeutic PTOA treatments that are more cartilage specific. This annual report details the portion (Aim 2: Determine the chondro-protective effect of locally delivered ZA using an animal model) of the grant being performed within the partnering-PI's lab (Price). This sub-project involves the pre-clinical testing of i.a. ZA injection for treating PTOA within a murine model of surgically induced PTOA (the DMM model). The purpose of this sub-project is to evaluate the *in vivo* mechanisms by which PTOA progresses within the DMM model and to establish the efficacy and mechanisms of action of i.a. ZA in preventing PTOA. This sub-project is establishing these properties through the measurement of the structural, morphological, biochemical, molecular, and cellular properties of cartilage and bone in mice treated with i.a. ZA following the induction of injury via the DMM model. Since the in situ repair of degenerate cartilage is a challenging, and a yet unrealized task, the prevention of PTOA through the innovative i.a. delivery of ZA may provide a simple, effective, and lower-cost treatment for lessening the burden of this disease. Furthermore, the knowledge of the chondro-protective mechanisms of ZA that may help to identify additional molecular, cellular, and biochemical targets by which OA/PTOA may be treated in the future.

2. **KEYWORDS:** Post-traumatic osteoarthritis; cartilage degeneration; DMM model; bisphosphonate; zoledronic acid; intra-articular injection; chondro-protection; cartilage therapy; anti-osteoarthritic.

3. **Accomplishments:** Within 2nd Aim (sub-project) of this grant "Determine the chondro-protective effect of locally delivered ZA using an animal model", of which the laboratory of the partnering-PI (C. Price) is responsible for, the following summary of major goals, accomplishments, training and professional are noted for this (7/15 to 6/16) and the previous reporting periods.

    a. Major goals of the project as state in the approved SOW (in table format).

Specific Aim 1: Investigate the "in vivo chondro-protective effects of zoledronic acid (ZA) – a small-animal (Mouse) model of surgically induced PTOA and treatment"	**Milestone achieved**
Major Task 1: Evaluate the in vivo chondro-protective efficacy of immediate and delayed targeted local administration of zoledronic acid (ZA) to prevent post-traumatic osteoarthritis (PTOA)	
Subtask 1: Obtain final IACUC/ACURO animal protocol approval and finalize PTOA surgery and intra-articular (i.a.) injection procedure development and training	*12/13*
Subtask 2: Perform PTOA surgery (DMM and Sham), i.a. injections (ZA and vehicle; peri- & post-operative), and animal sacrifice/specimen harvesting; procedures will be performed in a batch-wise manner	**3/16**

Animals Used: 383 Mice; Strain: C57BL/6J, [Jackson Labs]	
Subtask 3: Micro-computed tomography (micro-CT) imaging-based characterization of joint bone structure following PTOA surgery and i.a. ZA intervention.	**4/16**
Subtask 4: Histological characterization/assessment of articular cartilage damage/protection following PTOA surgery and i.a. ZA intervention.	**90% Complete**
Subtask 5: Immunohistochemical evaluation/characterization of cartilage cellular responses following PTOA surgery and i.a. ZA intervention.	**60% complete**
Major Task 2: Experiment Data Analysis, Yearly Reporting, and Publication	
Subtask 1: Ongoing analysis of data generated during study progression	**75% complete**
Subtask 2a: Yearly Report (Year 1)	*8/14*
Subtask 2b: Yearly Report (Year 2)	*8/15*
Subtask 2c: Yearly Report (Year 3)	**8/16**
Subtask 2c: Final Report (Year 4)	
Subtask 3: Publication of 2-3 peer-reviewed papers and 5-8 peer-reviewed conference proceedings disseminating investigations research	**33% complete**

b. Accomplishments under these goals.

1. Brief description of methodologies utilized within the present tasks:
    - *Surgery:* Adult, male C57BL/6 mice (Jackson Labs) underwent DMM-surgery in their right limbs at 12-weeks of age and were randomly separated into four groups: DMM with no treatment (DMM), DMM + an immediate single i.a. ZA injection, DMM + a single 1wk post-DMM i.a. ZA injection, DMM + i.a. ZA injections at 0-d, & 1-, 2-, and 3-wk post-DMM. i.a. ZA injections were administered at a dose of .64 ng/kg per injection (ZA monohydrate) based upon previous *in situ* work conducted by our collaborator.
    - *Sample processing:* Joints were harvested at 7-, 14-, 56-, and 84-days post-DMM (n=5-10 mice/group). For histological analysis, samples were fixed, decalcified, embedded in paraffin, and cut (5-μm thick coronal sections). Every 20th section (~100 μm apart) was stained with Safranin-O, fast green, and Weigert's iron hematoxylin. From these, five sections spanning the joint's mid-contact cartilage regions were selected for semi-quantitative scoring. The slides were labeled (1-5), from the anterior to posterior levels of the joint.
    - *Histological Scoring:* By using semi-quantitative histological scoring systems, three blinded individuals evaluated the severity of width-wise cartilage damage on a 0-6 scale, and the degree of synovitis and osteophyte formation/maturation on a 0-3 scale. Whole-joint damage, synovitis, and osteophyte scores were then derived for each specimen (averaged all sections).
    - *Immunohistochemistry:* Three sections spanning ~300-μm of the cartilage-on-cartilage contact were stained histologically and immunohistochemically to assess the progression of chondrocyte death and proliferation in the medial compartment tibial plateau. To determine chondrocyte viability, sections

were stained with hematoxylin and eosin (H&E; hematoxylin for cell chromatin/DNA), DAPI (intact cell DNA), and TUNEL assay (apoptosis). Chondrocyte proliferation was determined immunohistochemically via Ki-67. To quantitate chondrocyte changes, we used a custom, semi-automatic MATLAB algorithm to manually count positive cells for each stain in the medial tibia plateau (MTP) AC. The number of positive cells were automatically determined across four quadrants of the MTP AC width (quad 1 [inner most region of joint] through 4 [closest to joint margin]).

- *Quantification of Meniscal Coverage and Chondrocyte Presence:* To determine the spatial (medial-to-lateral) and temporal relationships between meniscal extrusion/coverage and chondrocyte cellularity and cartilage damage, we stained sections (immediately adjacent to the Safranin-O section) for type II collagen and DAPI-positive cells. Using a custom, semi-automated MATLAB algorithm, we traced the medial tibial plateau articular cartilage (AC), calcified cartilage (CC), and meniscus and counted the number of DAPI-positive cells in AC and CC (Fig. 2A). From these traces and counts, we determined the degree of meniscal coverage (length of meniscus/width of articular surface) and number of DAPI-positive cells in four quadrants (quad 1 [inner most region of joint] through 4 [closest to joint margin]) of the AC and CC.
- *μ-CT analysis:* For micro-CT (*μ*-CT) analysis, DMM, Sham, DMM + i.a. ZA, and contralateral joints were scanned using a *μ*-CT scanner (6um/voxel; Scanco uCT-35). To quantitate structural changes in calcified tissues, the calcified meniscus, intracapsular ectopic bone, subchondral bone, and epiphyseal bone were manually segmented from 3D images and processed using CTan software.

2. Within Task 1 "*Evaluate the in vivo chondro-protective efficacy of immediate and delayed targeted local administration of zoledronic acid (ZA) to prevent and post-traumatic osteoarthritis (PTOA) in a murine model of PTOA development"* we have completed the surgeries and collection of all animals specimens for the complete cohort of Baseline, Age-Matched, and SHAM controls, DMM Surgery + No Treatment, and DMM + i.a. ZA treatment groups with collections that were performed between post-surgery days 0 and 112.

During the reporting period we have performed 127 DMM surgeries and 40 i.a. injection procedures. Over the life of the award we have performed 155 DMM and 30 SHAM surgeries, and 214 i.a. ZA injections, and have utilized a total of 352 animals out of the total of 396 requested. All studies utilizing live animals have been completed (See Table #1) and no more live-animal studies will be conducted.

Table 1 **Animal Surgery and Specimen Collection Breakdown**

Experimental Grou	Surgery @ 12wks	i.a. ZA Treatment @	0d		3d		7d		14d		3wk		8wk		12wk		16wk		Total Mice	Animal Protocol Status
			Hist.	*u-CT*	*Hist.*	*u-CT*	*Hist.*	*u-CT*	*Hist.*	*u-CT*	*Hist.*	*u-CT*	*Hist.*	*u-CT*	*Hist.*	*u-CT*	*Hist.*	*u-CT*		
Baseline and Age-Matched Controls	N.A.	N.A.	5	5	-	-	-	-	-	-	-	-	5	5	5	5	5	5	40	**Complete**
Sham Controls	Sham	N.A.	-	-	3	2	3	2	3	2	-	-	3	2	3	2	3	2	30	**Complete**
Vehicle and ZA Controls?	N.A.	Vehc.	-	-	3	2	3	2	3	2	-	-	3	2	3	2	3	2	30	**Complete**
DMM Only	DMM	N.A.	-	-	5	5	5	5	5	5	-	-	10	5	10	5	10	5	75	**Complete**
DMM + Peri-Operative Tx	DMM	Day 0	-	-	-	-	5	5	5	5	-	-	10	5	10	5	10	5	65	**Complete**
DMM + Post-Operative Tx	DMM	Day 7	-	-	-	-	-	-	5	5	5	5	10	5	10	5	10	5	65	**Complete**
DMM + Multiple Tx	DMM	D0, 7, 14, 21	-	-	-	-	-	-	5	3	-	-	10	3	10	3	10	3	47	**Complete**

- = Not Applicable
Note: All animal protocols have been completed.

Total Mice Used **352**
Total Mice Budgeted **396**

Upon collection, ~2/3^{rds} of joint specimens (432; including both experimental and contralateral control knees) were processed for paraffin embedding, microtomy, histological scoring of cartilage damage, and immunohistochemical evaluation. Of these 100% of the specimens have been processed and embedded and 90% have been microtomed, stained, images and archived (44 remain to be analyzed; Table 2). In this study arm samples were processed in house for paraffin embedding for microtomy, thin sections were cut on a rotary microtome and prepared for the scoring of cartilage damage (3 individuals were trained on sample preparation). Scoring of cartilage damage involved the Safranin-O/Fast green/Weigert's Iron Hematonxylin staining of joint section, followed by semi-quantitative evaluation (based upon the OARSI-describe PTOA scoring system) by three blinded scores (5 individuals have been trained on cartilage scoring). Cartilage scoring data collection and

data analysis has been completed for the Baseline, Age-Matched, SHAM, DMM, and DMM + i.a. ZA cohorts (results described in Research Findings). Additionally, immunohistochemical (IHC) staining for the collagen/osteoarthritis relevant markers - collagen type II, collagen type X, Ki-67, and TUNEL have been completed for ~50% of the Baseline, Age-Matched, SHAM, DMM, and DMM + i.a. ZA cohorts and analysis is ongoing.

The remaining ~1/3rd of the specimens (272) were reserved for u-CT scanning and analysis, processing for plastic embedding and archiving (with a small subset of samples chosen for histomorphometric analysis). Of these all 272 have been u-CT scanned (in the UD DRI Cytomechanics Core Facility) and analyzed in house (Table 2), plastic embedding and archiving is ongoing, and histomorphometric analysis on a select subset of samples will be completed soon.

Table 2: Specimen Processing Progress

Analysis Arm	Collected Joints		Projected Joints	Analytical Task	Number Completed	% of Collected	% of Projected
Histology/IHC Arm	432	of	432	*Processing & Embedding*	*432*	*100%*	*100%*
				Microtomy	*388*	*90%*	*90%*
				Histological Staining	*388*	*90%*	*90%*
				OA Scoring	*388*	*90%*	*90%*
				*IHC Staining and Analysis**	*104*	*61%*	*61%*
				** – Project number of joint assayed by IHC (~170) is less than total projected*			
Micro-CT Arm	272	of	272	*u-CT Scanning and Analysis*	*272*	*100%*	*100%*
				Histomorphometric Processing	*Select Samples Currently in Processing*		
				Histomorphometry Analysis	*Awaiitng Completion of Prior Step*		

The PI notes, that at the present, all of the sub-tasks associated with Task #1, except for the final histological and IHC analysis of <10% of the i.a. ZA injection cohorts (exclusively the cohort controls) have been completed. The finalization of these studies are presently ongoing and we expect the completion of these analysis procedures within the next 4 months.

3. Within Task 2: "*Analysis of data; Preparation of annual and final reports, publication and grant proposal based on our findings.*" The analysis and dissemination of our research findings has been ongoing and is described below in section 3, ***Research Findings***. During the present reporting period we have published and presented our results regarding this research in the following venues: The University of Delaware's Center for Biomechanical Engineering Research 13th Annual Biomechanics Research Symposium, the University of Delaware's 7th Annual Graduate Student Forum, the 2016 Summer Biomechanics, Bioengineering and Biotransport Conference, the 2016 Musculoskeletal Biology and Engineering Gordon Conference. We are also planning to submit four (4) abstracts to the 2017 ORS and OARSI conferences. We have also prepared the first manuscript reporting data from this study; this manuscript details the early, focal changes in cartilage cellularity and structure that following the surgically induced meniscal destabilization of the mouse knee joint. This manuscript has been accepted for publication in the Journal of Orthopaedic Research with minor revisions, which we are in the process of submitting.

4. Research Findings: Some notable and reported highlights of our research findings so far are as follows:

Early, Focal Changes in Cartilage Cellularity and Structure Following Surgically-Induced Meniscal Destabilization in the Mouse – Histological analysis of mouse joints following DMM (control joints) has demonstrated the important findings of rapid (within 3-day of injury), and spatially localized (focal) changes in both the cellularity (loss of chondrocytes) and the structure integrity of articular cartilage. The findings shed new light onto the early natural pathology and time-course of PTOA development following DMM and suggest that acute changes to a focal population of chondrocytes and region of articular cartilage tissue may be critical in the initiation of long-term cartilage degeneration following joint injury and represent a potential target for

chondo-protective/anti-osteoarthritic therapy. The findings are highlighted in the following figures and descriptions (**Fig 1 - 7**) findings which have been accepted for publication in the Journal of Orthopaedic Research with minor revisions.

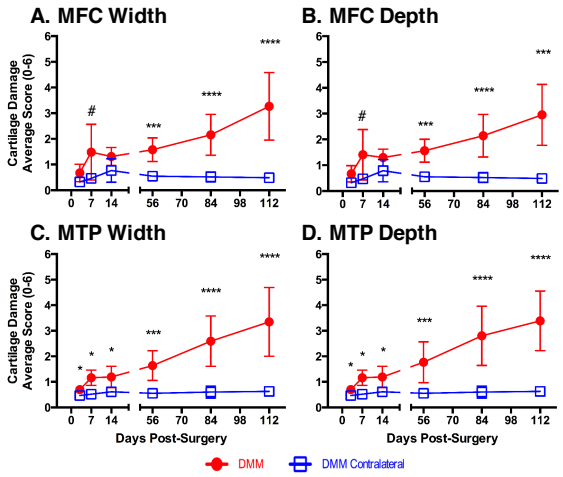

Figure 1: Semi-quantitative histological scoring of the whole mouse joint demonstrated the rapid accumulation of significant proteoglycan loss and surface fibrillations [scores = .5-1] as early as 3-days in DMM joints, which then stabilized between 7- and 56-days as surface fibrillations and clefts [scores = 1-2], before progressing into larger width-wise (C.) and depth-wise (D.) erosions [scores ≥3]. Similar trends were observed for the MFC (A. and B). These results illustrate the rapid nature of post-injury changes within mouse knees subjected to DMM surgery. However, they do not indicate how the damage progresses spatially within the joint following injury, nor how these changes correlate spatially with other joint level changes following DMM.

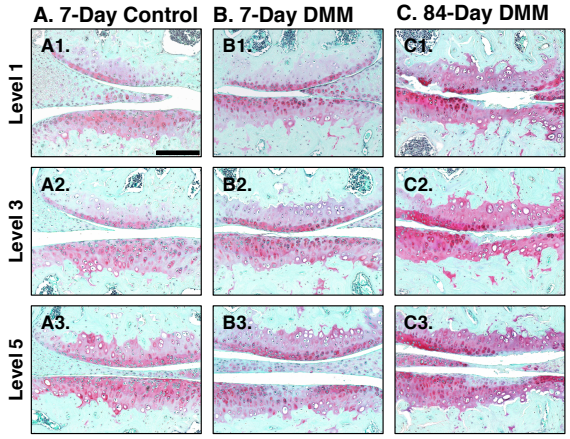

Figure 2: Safranin-O staining of sections qualitatively highlighted the spatial and temporal changes that occur to the joint following DMM-injury. The medial meniscus was observed to extrude toward the medial margins of the joint resulting in the uncovering of previously covered tibial plateau and femoral condyle articular cartilage that is more pronounced anteriorly and in the center of the contact medial-laterally. These changes appeared to coincide with bot the distribution of cartilage damage from the anterior (level 1), through mid-contact (level 3) and posterior (level 5) levels of the joint as well as medial laterally within the joint suggesting that the movement of the meniscus is critical factor in the initiation and location of cartilage damage following DMM.

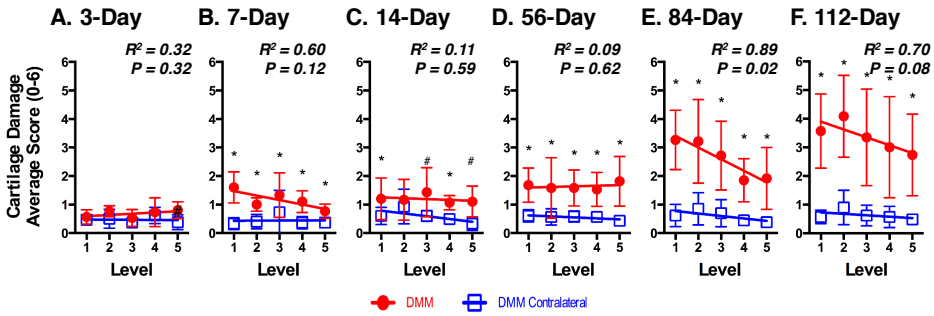

Figure 3: Semi-quantitative scoring of cartilage damage in the medial femoral condyle confirmed the preferential anterior (level 1) vs. posterior (level 5) localization of cartilage damage that we observed visually following DMM-injury.

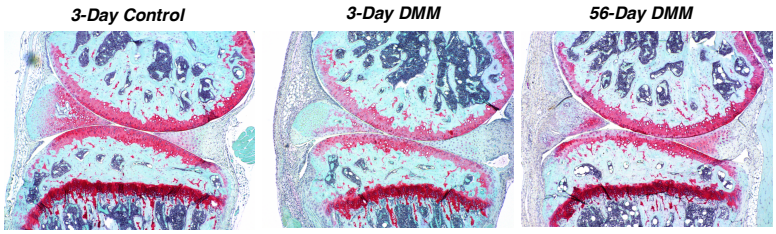

Figure 4: A subset of injured DMM and DMM contralateral joints that were sagittally sectioned and stained with Safranin-O/fast green to visual entire anterior-to-posterior and medial-to-lateral progression of cartilage damage confirmed these findings.

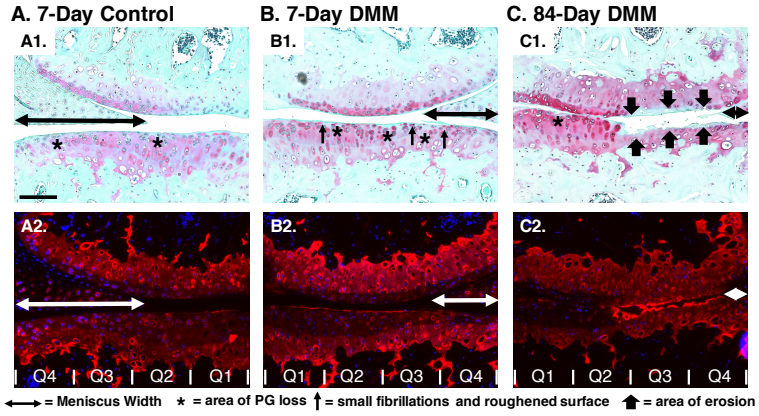

Figure 5: Adjacent histological (Safranin-O/fast green [upper panel]) and immunohistochemical (type II collagen and DAPI [lower pane]) illustrated a distinct loss of both proteoglycan staining as well as chondrocyte presence and increased type II collagen staining in regions of the MTP cartilage that col-localized with those the also experienced a loss of meniscal coverage (specifically Quadrant 3 [Q3]). These findings again suggest the importance of injury-related changes in the meniscus on cartilage contact that appear to precipitate compositional, cellular and structural changes in cartilage that lead to PTOA.

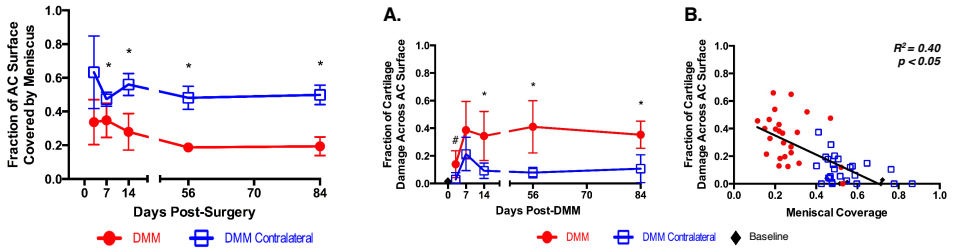

Figure 6: Quantification of changes in the extend of meniscal coverage following DMM and the extent of articular cartilage damage following DMM illustrate the strong correlation between surface damage and the extrusion of the medial meniscus. Confirming the quantitative observations above.

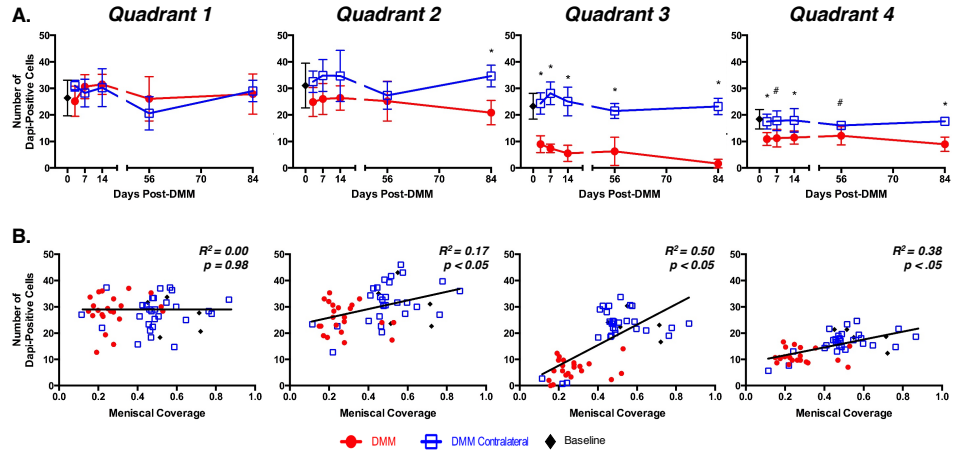

Figure 7: Measurement of the presence of chondrocytes spatially across the medial tibial plateau following DMM, and the relationship between changes in chondrocyte presence and the extent of meniscal extrusion illustrates the link between changes in the configuration of the joint post-DMM and the initiation of degenerative cellular changes. Following DMM, extensive chondrocyte loss was rapidly observed within the articular cartilage quadrant that experience acute and chronic meniscal uncovering (Q3), with loss only spreading to adjacent region (Q2 and 4) at later time points. This finding and the strong correlation between chondrocyte presence and meniscal coverage in quadrant 3 (and to a lesser degree Q2 & 4) highlights the importance of a stable joint in maintain the cellular and structural health of the joint. These findings also suggest that the focal loss of chondrocyte within Q3 following DMM may constitute the acute precipitating event that initiated the progression of PTOA. As such these cells now appear to be a specific target for the direct study of, as well and leveraging therapeutic strategies against.

DMM Induces Rapid and Focal Progression of Chondrocyte Proliferation and Apoptosis: Based upon extensive histological and immunohistochemical investiagation of mouse joints following DMM-injury we observed the appearance of a distinct spatiotemporal progression of chondrocyte proliferation and apoptosis, which is suggestive of the focal activation of endochondral ossification like process with the articular cartilage following acute injury.

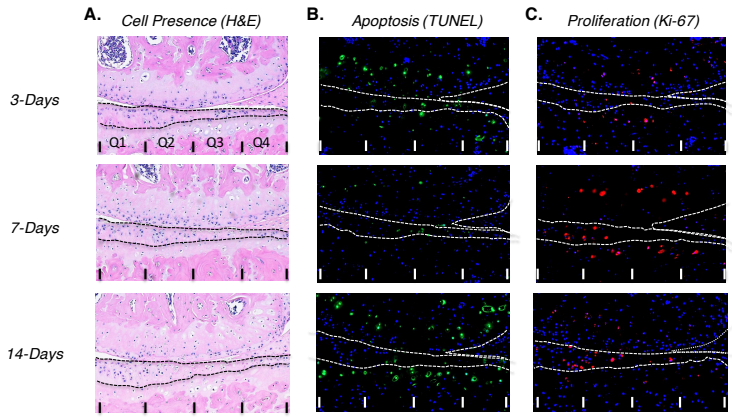

Figure 8: An immediate (within 3-days) reduction in chondrocyte number was seen by H&E and DAPI in regions where the AC experienced acute altered femur-on-meniscus-on-tibia contact following injury (Q3). In these regions TUNEL staining co-localized with areas lacking DAPI-positive cells, consistent with these cells undergoing apoptosis. We also noted that from 3-days onward a spatiotemporal progression of proliferation and apoptosis was observed. Tissue regions initially exhibiting increased Ki67 expression (proliferation) at early timepoints subsequently exhibited increased TUNEL positive staining (apoptosis) and loss of chondrocytes, resulting in the lockstep spread of chondrocyte proliferation then apoptosis and cell loss to adjacent AC quadrants. Based upon these findings we suggest that chondrocyte proliferation may be a key, albeit detrimental, injury-response mechanism. We posit that altered loading patterns can activate chondrocyte proliferation and endochondral progression in chondrocytes. However, the production of matrix degrading enzymes and paracrine factors required to support these processes may further accelerate the degradation of an AC extracellular matrix that is already under aberrant mechanical loading, contributing to the vicious cycle of cartilage degeneration.

Whole-Joint Structural Consequences Following Destabilization of the Medial Meniscus in the Mouse – Both histological and micro-CT analysis also demonstrated the presence of significant whole joint structural changes that occur within the knee joint following DMM surgery. Some of these like synovitis and osteophyte development occur very rapidly and are key components of the early, natural pathology of the joint following injury. While others (enlargement and remodeling of the injured meniscus and the ectopic calcification of the joint capsule occur later in the disease progression, and have heretofore been overlooked in the study of this injury model.

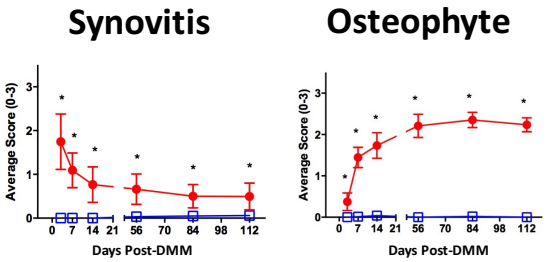

Figure 9: Synovitis is defined as inflammation of the synovial membrane that lines the cavities of synovial joints, and may play a role in the development of osteoarthritis. We have observed that in DMM-joints, but not in SHAM or control joints, that synovitis spikes rapidly (by 3-days post injury) then slowly subsides, but does not disappear, over the course of the study. Additionally, osteophytes, which are boney spurs that form along

joint margins and represent areas of new cartilage and bone, formed through endochondral ossification, may also play a role in in situ tissue repair, joint stabilization, and possibly disease progression. He we have shown that osteophyte development, through the formation of a cartilage template the subsequently undergoes calcification and bone formation, occurs very rapidly following DMM-injury as well. In both of these cases the extent of changes in the DMM model have been historically under-appreciated due to the fact that previous studies of joint structure in the DMM model in mice have largely focused on the late stage pathology of the disease.

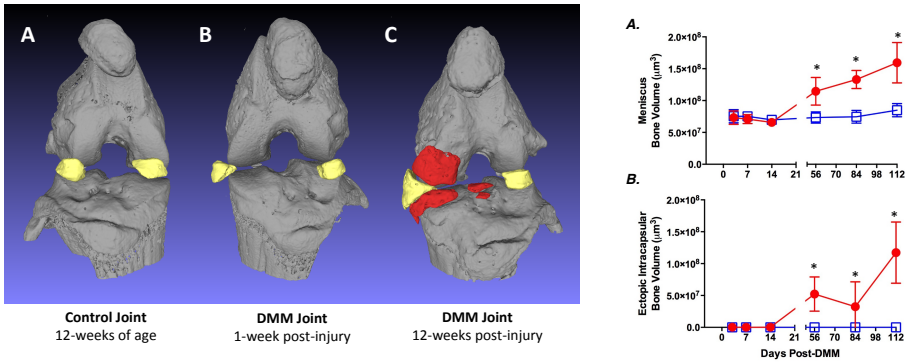

Figure 10: Micro-CT analysis of the DMM joints demonstrate the presence of long-term, gross morphological changes in presence and structure of intra-capsular calcified tissues. In healthy mice only the anterior and posterior menisci on the medial and lateral sides of the joint are calcified (yellow). Immediately following DMM, the menisci are see to extrude medially from the joint contact, and at later time points are observed to undergo significant increase in tissue and bone volume and drastic changes in morphology. Similarly, in DMM joints we observed the significant development of ectopic calcifications within the anterior-medial compartment of the joint at 56-days post-DMM and beyond. These changes were not observed in SHAM and Control joints and have been previously unreported in the literature. We suggest that these observed increases in tissue calcification may represent a previous unrecognized response in the mouse knee to attempt to re-stabilize the joint following injury.

Repeated Intra-Articular Injection of Zoledronic Acid Suppresses Cartilage Erosions Following Destabilization of the Medial Meniscus in Mice – Systemically delivered, high-dose ZA has demonstrated anti-osteoarthritic efficacy in animal models, including the murine destabilization of the medial meniscus (DMM) model. Nonetheless, the risk of significant skeletal side-effects due to high-dose nBP treatment represents a barrier to the clinical acceptance of systemically delivered nBPs for preventing PTOA. However, recent work has shown that ZA can have direct, beneficial effects on the metabolism and health of chondrocytes in situ. These results suggest that local targeting BPs to the joint, e.g. via direct intra-articular (i.a.) injection, may represent an alternative strategy for utilizing nBPs to prevent PTOA; yet, the application of nBPS in this manner has been nascent. We hypothesized that i.a. injection of nBPs, through their direct chondroprotective and anti-inflammatory activities, will suppress cartilage damage and degenerative joint changes following joint injury. Therefore, the objective of this study was to determine the efficacy of i.a. injection of the nBP ZA as an anti-osteoarthritic therapeutic in the murine DMM model of PTOA. Studies of joint changes in DMM mice that have been administered intra-articular (i.a.) injection of ZA demonstrate the ability of repeated i.a. ZA to provide a degree of anti-osteoarthritic activity within the mouse joint.

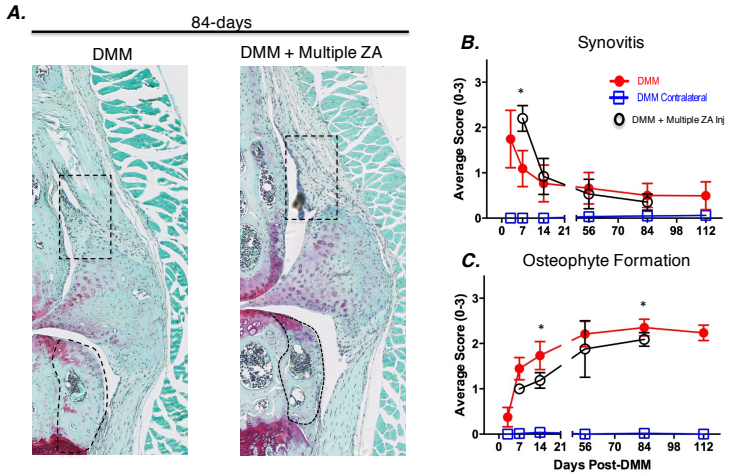

Figure 11: Both single (day 0 or day 7 injection) and repeated i.a. ZA injections (day 0, 7, 14, and 21) failed to ameliorate the development and degree of synovial inflammation post-DMM. Single i.a. administration of ZA to the joints likewise did not have a substantial effect on the long term development of osteophytes within the joint (data not shown). However, multiple i.a. injections of ZA tended to delay osteophyte maturation (seen as delay in the transition from a cartilaginous tissue to calcified bone) throughout the study.

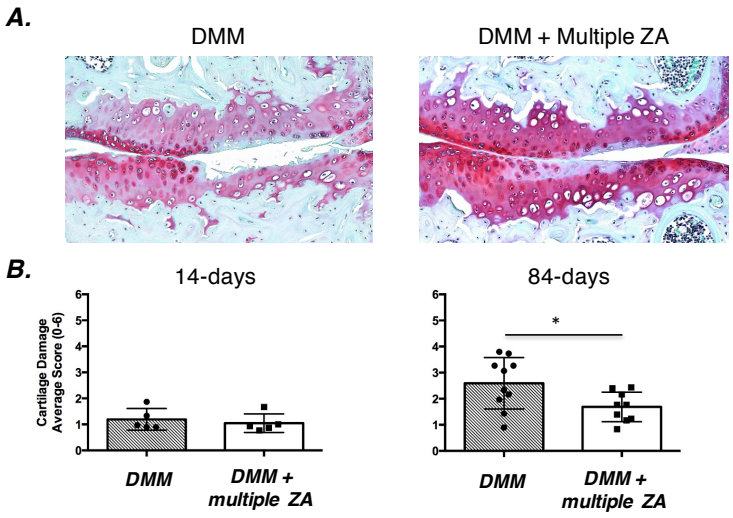

Figure 12: Histological studies of cartilage changes following DMM-injury and the administration of i.a. ZA demonstrated that only repeated i.a. ZA injections provided a significant degree of long-term anti-osteoarthritic efficacy. While multiple i.a. injections of ZA were unable to ameliorate the early progression of superficial cartilage damage, they were able to significantly suppress the cartilage erosions typically seen in untreated joints at later time points (84-days). These findings establish a framework to investigate the *in vivo* mechanisms underlying the efficacy of i.a. ZA in treating PTOA, and demonstrate the promise that i.a. ZA holds for the clinical translation of i.a. ZA in treating PTOA.

Conclusion – The work completed to date in this award has shed new light into the pathology and natural course of post-traumatic osteoarthritis (PTOA) as well as the potential for the use of intra-articular injection of the FDA-approve bisphosphonate zoledronic acid in the treatment of PTOA. Joint injury is a major occupation

hazard of military training and service, as well as athletic and recreational endeavors. A long-term consequence of joint injury is PTOA. Up to 50% of patients that suffer traumatic joint injury will will go on to develop PTOA and subsequent physical disability within 10 to 15-years of initial injury. We have made substantial progress toward the primary goal of this award, to investigate the therapeutic potential of a novel, intra-articularly injected drug therapy, zoledronic acid, to prevent PTOA development using a small animal model of knee injury. Through our pre-clinical mouse injury model we have established that changes in joint health, including cartilage composition and structure, and joint morphology appear very quickly following injury and are driven by very focal changes in chondrocyte health. In our animal model these changes are seen as early as 3-days post-injury and it is not unreasonable to assume that similar early changes are occurring clinically in human patient that have experienced traumatic joint injury. We have also demonstrated that while a single i.a. injection of ZA post-injury does not provide anti-osteoarthritic benefits in the mouse DMM-model of PTOA, multiple injections (4) over the course of 21-days does provide a degree of protection against cartilage damage.

At the present we have met the vast majority of the goals stated. We have successfully completed all of the indicated animal studies, ad have concluded all animal protocols associated with the present study. We have also completed over 90% of the required histological analysis and over 50% of the required IHC analysis. We will complete the remainder of this analysis fill out full coverage of our experimental and control groupings. We have also completed 100% of the micro-CT studies required. One goal that we have not met pertains to the biomechanical testing of the murine cartilage following DMM and therapeutic treatment. We had developed an indentation testing system with the help of our collaborators in Mechanical Engineering; however, we found through preliminary studies that the testing system did not have sufficient sensitivity to allow the quantification of changes in mouse cartilage mechanical properties due to injury and treatment. The samples that were reserved for testing have been retained in the hope that a more sensitive testing strategy can be developed in the future to permit such analysis. However, given the striking changes that we observed in the histological and immunohistochemical analysis we are confident that our results are compelling in the absence of these mechanical testing data. With regards to the other stated goals, the only ones that we have not fully completed involve the final analysis of data and the full dissemination of the either research docket through peer-reviewed publication. We are presently preparing 3 manuscripts that will present this entire body of work to the field and we expect to have them completed and submitted within the timeframe of the 1-year no cost extension that was granted.

c. Opportunities for training and professional development provided by the project.

The following students, staff, and faculty were provided training opportunities through this award during the reporting period.

Graduate Student Training:

Michael David – University of Delaware Biomedical Engineering Graduate Student (3rd-year Ph.D. Student; student lead on project; supported by award)

Brian Graham – University of Delaware Mechanical Engineering Graduate Student (3rd-year Ph.D. Student; assistance with data analysis)

Janty Shoga – University of Delaware Biomechanics and Movement Science Graduate Student (M.Sc. Student Graduated 7/2016; assistance with data analysis)

Ryan McDonough - University of Delaware Biomedical Engineering Graduate Student (1st-year Ph.D. Student; assistance with imaging and data analysis)

Undergraduate Student Training:

Avery White - University of Delaware Biomedical Engineering Undergrad (Graduated 6/2016 Spring 2016)

Rachel Pilachowski - University of Delaware Biomedical Engineering Undergrad (Junior Fall 2015 – Summer 2016)

Sejal Shah - University of Delaware Biomedical Engineering Undergrad (Freshman Summer 2016)

Alexis Merritt - University of Delaware Biomedical Engineering Undergrad (Sophomore Spring and Summer 2016)

Christopher Hernandez - University of Delaware Biomedical Engineering Undergrad (Sophomore Fall and Spring 2016)

Malhar Sakarwala - University of Delaware Biomedical Engineering Undergrad (Sophomore Spring 2016)

Srinivasa Gajjala - University of Delaware Biomedical Engineering Undergrad (Sophomore Spring 2016)

High School Student Training:

Shu-Jin Kust – Charter School of Newark DE Rising Junior (UD Summer 2016 K12 Program)

Michael Lan – Wilmington Charter School, DE Rising Senior (UD Summer 2016 K12 Program)

Staff Training:

Melanie Smith – Research Technician University of Delaware Biomedical Engineering (staff lead on project; partially supported by award)

Faculty Training:

Christopher Price – Assistant Research Professor, University of Delaware Biomedical Engineering (PI on project) – During the reporting period Dr. Price attended the University of Pennsylvania's Cartilage Repair Symposium in Philadelphia, PA and the 2016 Summer Biomechanics, Bioengineering, and Biotransport Conference in National Harbor, MD to increase his knowledge in the field of cartilage biology and repair, and orthopaedic biomechanics, respectively

d. Results Disseminated – Results of the research were disseminated to the general public in two ways: First, through the incorporation of research methodologies and research findings in the Biomedical Engineering core curriculum course that the PI (Price) teaches at the University of Delaware. Examples of the socioeconomic concerns of PTOA and the present findings of the PI's research in PTOA funded by this award were incorporate into the course lecture on the pathophysiology of the musculoskeletal system. Second, research images produced through the present project were displayed at the 1st Annual Since in Art Symposium at the University of Delaware in April of 2016. The symposium was sponsored by the UD BME Department and highlighted the research work being performed at the University through the display and discussion of artistic images produced through research. Three students present 5 pictures that were derived from the present work.

e. Plans during the next reporting period to accomplish the goals – During the next reporting period the PI will oversee the final experimental processing and analysis of the remaining outstanding histological and IHC specimens to complete the proposed study. The PI will also direct the final collation and analysis of the DMM and DMM + i.a. ZA data sets for the preparation of publication. This will include the final collection, the statistical analysis and the final interpretation of these data. The PI will oversee the writing and preparation of a minimum of three manuscripts that will disseminate the final result of the research to the filed through peer-reviewed publication. The PI will also oversee the preparation and submission of conference abstract relevant to the present research; this includes 4 abstract submissions to the 2017 Annual Meeting of the Orthopaedics Research Society, as well as submission to the OA International Research Society Meeting, the 2017 SB3C, and numerous local and regional symposium.

4. **Impacts:** Within 2nd Aim (sub-project) of this grant the following distinctive contributions, major accomplishments, innovations, successes, and changes in practice or behavior have come about as a result of the project.

   a. Impact of development of the principal disciplines(s) of the project.

1. As a result of the findings of this research, we and the field of PTOA biology now have an increased appreciation for the early and focal changes in cellular health that accompany the destabilization of the joint following acute injury. We have demonstrated the critical role that the configuration of the meniscus plays in the initiation and progression of chondrocyte death and cartilage structural changes following injury.

2. We have also demonstrated within the present PTOA model the rapidity and focal nature of chondrocyte death following injury. These findings now present a distinct population of against which the study of disease progression and the molecular and cellular level can now be directed. In addition, the behavior of this population of cells indicates that these cells may be the focal initiators of PTOA development and progression and may constitute a population of cells (and pathology) that be targeted via chondro-protective (or anti-osteoarthritic) therapies to try to delay or prevent their death and the subsequent tissue degeneration.

3. These findings, identified in a small animal model of PTOA, have distinct similarities/correlates to processes observed in larger models as well as clinically in humans. Therefore, the specific processes and results identified herein can guide the investigation of similar PTOA pathologies within larger pre-clinical injury models, as well as in the clinical diagnosis and understanding of PTOA following acute knee injury.

4. We have also demonstrated that intra-articular injections of zoledronic acid, if administered repeatedly (weekly) following joint injury in the present model can provide a degree of anti-osteoarthritic efficacy. These findings support and corroborate ex vivo and in vitro findings from our collaborator, and highlight the potential for i.a. ZA as a therapeutic approach for mitigating the long-term effects of knee-injury on PTOA. These results support the further pre-clinical investigation of the present findings and the need for continued translational studies to refine the use of i.a. ZA as a PTOA therapeutic.

b. Impact on other disciplines.

1. While not yet directly applicable to the treatment of cartilage damage clinically following joint injury, these findings highlight the need to consider the immediate/acute changes occurring to the joint following injury in both the clinical study and care of patients. These results suggest that due consideration to the needs of joint stability following injury should be considered by clinical practitioners in the treatment and care of injured patients/service member. These findings also suggest that further research into the immediate post-injury changes within the knee should be a clinical priority, thus defining the timeline and specific pathophysiology of the disease in the clinical population. We suspect that a similar etiology should present clinically and would be a critical piece of knowledge in directing the treatment of joint injury in the attermpt to prevent long-term PTOA.

c. *Impact on technology transfer* – Nothing to Report

d. Impact on society beyond science and technology –

1. Ultimately, we hope that this basic science and translational research can lead to breakthroughs in the development of clinical treatments strategies that can be applied to the patients in the general population that suffer joint injuries in order to begin to relieve the significant socioeconomic burden of PTOA.

5. **Changes/Problems:** Within 2nd Aim (sub-project) of this grant the following instances of changes and/or problems are noted.

a. *Changes in approach*. - Nothing to Report

b. Actual or anticipated problems or delays. – During the performance of the stated goals we only encountered minor delays in concluding the histological and immunohistochemical analysis of samples associated with the DMM + i.a. ZA treatment groups. We have completed over 90% of all of the histological analysis of the data and prioritized the completion of the actual intervention groups to accelerate the dissemination of these data. At the present the remaining 10% of the samples that require analysis, and are delayed slightly (~4-months) compared to the statement of work, are currently being processed. The cause of this delay was just an issue of experimental volume and required more time to complete due to the delay in the initiation of some of the final animal studies outlines in the previous reporting period. With regards to the IHC analysis, the completion of the analysis had been delayed (~4-months) due to unforeseen issues in optimizing the protocols for the IHC staining of the collected samples. The optimization of the staining took longer than originally anticipated, however the procedures are now fully functional and the data is currently being collected. Presently, we do not anticipate any further delays in the performance and conclusion of the indicated studies and expect their completion by the scheduled conclusion of the no-cost extension granted to this award.

c. *Changes that had a significant impact on expenditures* - Nothing to Report

d. *Significant changes in use or care of human subjects* – Not Applicable

e. *Significant changes in use or care of vertebrate animals, biohazards, and/or select agents* - Nothing to Report

f. *Significant changes in use or care of biohazards, and/or select agents* - Nothing to Report

6. **Products:** The following products resulted from the project during the previous reporting period.

Publications, conference papers, and presentations

a. Journal Publications

1. David, MA, Smith, MK, Pilachowski, RN, White, AT,. Locke, RC, Price, C Early, Focal Changes in Cartilage Cellularity and Structure Following Surgically-Induced Meniscal Destabilization in the Mouse (Submitted and Accepted with Revisions to the Journal of Orthopaedic Research 2016)

b. *Books or other non-periodical, one-time publications* - Nothing to Report

c. Other publication, conference papers, and presentations

1. David, M.A., White, A.T., Pilachowski, R.N., Locke, R.C., Smith, M.K., Price, C. (2016) Spatio-Temporal Quantification of Cartilage Structural Changes in a Murine Model of Post-Traumatic Osteoarthritis, Summer Biomechanics, Bioengineering and Biotransport Conference (SB3C). National Harbor, MD. June 2016 (Podium Presentation)
2. David, M., Smith, M., White, A., Locke, R., Price, C. (2015) Quantification of Early Structural Joint Changes in a Murine Model of Post-Traumatic Osteoarthritis. Biomedical Engineering Research Society Annual Meeting. Tampa, FL. October 2015 (Poster Presentation)
3. White, A., David, M., Smith, M., Pilachowski, R., Price, C. (2015) Post-traumatic Osteoarthritis Dual Quantification System of Cartilage Degradation in Murine Model Following Joint Destabilizing Surgery. Biomedical Engineering Research Society Annual Meeting. Tampa, FL. October 2015 (Undergraduate Poster Presentation)

4. David, M., Smith, M., Pilachowski, R.N., White, A., Locke, R., Price, C. (2016) Destabilization of the Medial Meniscus in Mice Induces Early, Localized Chondrocyte Loss and Cartilage Damage. Center for Biomechanical Engineering Research. University od Delaware. Newark, DE. April 2016 (Poster Presentation)

d. *Website(s) or other internet site(s)* – Nothing to Report

e. *Technologies or techniques* –

1. The destabilized medial meniscus (DMM) was perfected in the lab and is now routinely performed by the research staff in the lab and can be transferred/taught to other researchers.
2. We have modified the intra-articular (i.a.) injection protocol to reduce the invasiveness and precisely control the delivery of injectable administered. The technique is now routinely performed by the research staff in the lab and can be transferred/taught to other researchers.
3. Micro-CT analysis protocols have been developed and validated for murine knee joints on the Scanco u-35 system.
4. A modified OARSI-based PTOA scoring system was implemented within the laboratory with multiple researchers being trained on its use, and these scoring techniques will be published in a upcoming manuscript in the Journal of Orthopaedic Research.

f. *Inventions, patent applications, and/or licenses* - Nothing to Report

g. *Other Products* –

Degrees Obtained

- The following undergraduate students performed research supported by this award during the reporting period that count(ed) toward credit for graduation (Biomedical Engineering Independent Study Project)
  - Rachael Pilachowski (3cr. – Winter 2016; Cartilage scoring project)
  - Avery White (1cr. – Spring 2016; Cartilage scoring project)

Funding Applied for Based Upon Work

- In August 2015 I submitted a DoD CDMRP PRORP Applied Research Award pre-application that expanded upon the research that has supported by the present award. This proposal seeked to expand and validate the safety and pre-clinical therapeutic potential of i.a. ZA in combination with a biodegradable, controlled release drug delivery platform. This proposal was invited for full application but was not funded.
- In May of 2016 I submitted an Arthritis National Research Foundation Grant that expanded upon the research that has supported by the present award through the development and testing of controlled release delivery platforms for the i.a. administration of ZA to injured joints. This proposal was not funded.
- In July of 2016 I submitted a ACCEL Delaware Clinical Translation Grant to develop a liposomal based drug delivery platform with multiple functionalities for target delivery of ZA to the injured joint. This award is still pending.
- In September 2016 I will be submitting a DoD CDMRP PRORP Applied Research Award pre-application that expands upon the research that has supported by the present award.

7. *Participants & Other Collaborating Organizations*

a. *Individuals that have worked on the project* – Nothing to Report

b. *Change in the active support of the PD/PI(d) or senior/key personnel since last reporting period*

During the reporting period the following active grants have closed.

- NIH R21 - 1R21AR062738-02 (PI: Price) Dates: 4/1/2013 – 3/31/2016
- University of Delaware Research Foundation Award - 14A00762 (PI: Price) Dates: 6/1/2014 – 7/31/2016
- University of Delaware Research Foundation Strategic Initiative (PI: Price) (not funded)

During the reporting period the following active grants have been awarded.

- NSF CMMI BMMB - Proposal Number 1635536 (PI: Price) Awarded: to start 9/1/2016 – 8/31/2019

c. *Other organization involved as partners* – Nothing to Report

8. *Special Reporting Requirements*
   a. *Collaborative Awards – The present progress report outlines the tasks and progress that have been made by the Partnering-PI (Price) in the completion the indicated award. A separate progress report has been submitted by the project PI (Lu).*

9. *Appendices – N.A.*

Accepted for Publication (with minor revisions) Journal of Orthopaedic Research

Title: Early, Focal Changes in Cartilage Cellularity and Structure Following Surgically-Induced Meniscal Destabilization in the Mouse

Authors: Michael A. David, Melanie K. Smith, Rachael N. Pilachowski, Avery T. White, Ryan C. Locke, Christopher Price

Affiliations: Department of Biomedical Engineering, University of Delaware, Newark, Delaware, United States[1]

Corresponding Author:
Christopher Price
161 Colburn Lab, University of Delaware, Newark, DE 19716
Tel: +1 302-831-1147; e-mail: cprice@udel.edu

Type of Manuscript: Full length original research article

Author Contributions: All authors have read and approved the final submission of the manuscript. The contribution of the authors are described below:

Study Design – MAD, MKS, CP

Animal Research – MAD, MKS

Acquisition of Data – MAD, MKS, RNP, ATW, RCL

Analysis and Interpretation – MAD, CP

Manuscript Preparation – MAD, MKS, CP

Statistical Analysis – MAD

Running title: (5 word or less) Spatiotemporal Cartilage Changes Following DMM

Abstract:

Post-traumatic osteoarthritis (PTOA) is an accelerated form of osteoarthritic cartilage degeneration affecting approximately 50% of patients experiencing joint injury. Currently PTOA is incurable; to better understand the etiology of PTOA and to develop rational anti-osteoarthritic therapies, it is critical to understand the spatiotemporal initiation and the progression of PTOA. In this study, we employed semi-quantitative histological scoring and quantitative damage analysis to examine disease progression in the murine destabilization of the medial meniscus (DMM) model of PTOA from early- (3-days) through late- (112-days) disease time-points. We observed significant, progressive articular cartilage changes in the medial compartments of injured joints as early as 3-days. Damage was found to preferentially localize towards the anterior regions of the joint, and furthermore, a drastic loss in chondrocyte number (by 3-days), surface damage (at 7-days), and cartilage erosion (at 84-days) was found to co-localize to a small, focal region of the articular cartilage of the medial tibial plateau that experienced a change in meniscal coverage due to meniscal extrusion following DMM-surgery. Taken together, these results suggest that DMM-mediated extrusion of the medial meniscus leads to rapid, spatially-dependent changes in articular cartilage cellularity and structure, and precipitates the focal degeneration of cartilage associated with PTOA. Importantly, this study suggests that joint instability injuries may trigger immediate (<3 days) processes within a small population of chondrocytes that directs the initiation and progression of PTOA, and that development of chondroprotective strategies for preventing and/or delaying PTOA-related cartilage degeneration are best targeted toward these immediately-early processes following joint injury.

Abstract length = 250 words.

48 **Keywords:** Post-traumatic osteoarthritis, spatiotemporal cartilage damage, chondrocyte loss,

49 meniscal extrusion, Destabilization of the medial meniscus (DMM)

50

51 Manuscript length = 4151 words.

Introduction:

Nearly 50% of patients suffering a traumatic joint injury, e.g., anterior cruciate ligament tears, meniscal tears, or meniscectomies, will develop post-traumatic osteoarthritis (PTOA) within 10-15 years of their injury[1]. Currently, PTOA is not preventable and the precise mechanisms by which acute joint injury leads to long-term cartilage degeneration remains unknown[2] partly due to: i) limited availability of early disease stage human cartilage, ii) limited in vivo cartilage assessment techniques, and iii) the long timespan of clinical disease progression. To overcome these limitations and to define the mechanisms underpinning PTOA initiation and progression, cartilage degeneration has been studied in numerous pre-clinical small-animal models of joint injury.

The destabilization of the medial meniscus (DMM), a surgically-induced joint instability model, is considered a gold-standard PTOA model due to its ease of implementation, high reproducibility, and pattern of disease progression thought to closely recapitulate human osteoarthritis[3]. Collectively, murine DMM studies have identified mild cartilage damage in early-disease (7- and 14-days)[4–9] and mild-to-severe cartilage loss/erosion at mid-to-late stage disease (28 through 112-days)[9–22]. Typically, cartilage damage severity and progression have been evaluated using whole joint-level semi-quantitative histological scoring systems[20,23–25]. However, such systems have limited ability to fully characterize early changes in articular cartilage degeneration because they rely on: i) binary metrics of superficial tissue damage (fibrillations and clefts), which only indicate the presence of these changes not their spatial extent, and ii) metrics of cartilage erosion that simultaneously incorporate of width-wise (across the surface) and depth-wise (into the tissue) damage components in their analysis. Furthermore, scores are oftentimes presented as a single aggregated damage metric derived from the maximal extent of damage within a section(s) and joint compartment or summed/averaged across the joint.

Thus, while semi-quantitative scoring systems have helped to define the time-course of whole-joint level cartilage damage post-DMM, they can inadvertently mask key aspects of the spatial initiation and progression of cartilage degradation.

Defining the anterior-to-posterior and medial-to-lateral distribution of cartilage damage may provide critical insight into the mechanisms by which PTOA initiates and progresses. In the pioneering DMM study by Glasson et al.[3], qualitative observations of spatially-dependent cartilage damage, specifically a preference for anteriorly-directed damage within the medial tibial plateau of DMM-joints, were found. Furthermore, while not addressed in prior studies, our qualitative impressions of the murine DMM literature suggests a co-localization of cartilage damage to medial regions of the tibial plateau that were previously covered by the medial meniscus[7,9,14–16,20–22,26,27]. Supporting these impressions, studies utilizing DMM within various species have indicated increased joint laxity and anterior translation (mice)[28], altered medial compartment contact stresses (mice and rabbit)[10,29], and cartilage damage to the middle and outer medial tibial plateau (rat)[30]. Furthermore, non-invasive murine models of PTOA support the co-localization of applied load, cartilage damage, and chondrocyte apotosis[31]. While a few murine studies have identified increased chondrocyte death post-DMM[4,6,24,26,32], the details regarding the spatial distribution of chondrocyte loss across the articular cartilage and their relationship to meniscal extrusion have yet to be investigated.

Taken together, we believe that meniscal extrusion post-DMM plays an important role in the rapid, focal initiation and progression of cartilage damage. We hypothesized that chondrocyte loss and cartilage structural damage would rapidly (≤7-days) and preferentially localize to cartilage regions where DMM-induced medial meniscus extrusion results in altered femur-on-meniscus-on-tibia contact. However, the use of conventional semi-quantitative scoring alone

would likely be unable to address such relationships. Therefore, we utilized a set of spatiotemporal scoring and evaluation methods to address this hypothesis and to elucidate the relationship between meniscal extrusion and changes in cartilage cellularity and structure from early (3-day) through late-stage (112-days) disease in the murine DMM model of PTOA.

Methods

Animals and Surgeries: Male C57BL/6 mice (n = 83) were purchased from the Jackson Laboratory at 9-weeks of age and housed in standard cages (≤5 mice/cage). Mice were maintained on a 12-hour light-dark cycle in a climate controlled vivarium with access to food (Prolab RMH 3000) and water *ad libitum*. Mice were randomly assigned to one of three groups: DMM, sham, or baseline/age-matched controls.

At 12-weeks of age, right knees of mice in the DMM group (n = 5-10 mice/group) underwent the DMM surgery[3,21]; contralateral limbs served as un-operated internal controls. Briefly, mice were anesthetized using inhaled isoflurane and prophylactically administered antibiotic and analgesic. Using aseptic techniques, the medial meniscotibial ligament (MMTL) was exposed and transected to release the anterior horn of the medial meniscus from the tibia and then surgical incisions were subsequently closed. A subset of mice underwent sham surgery, identical to the DMM surgery, except transection of the MMTL was omitted. Following surgery, mice recovered quickly to full ambulation and unrestricted cage activity. Collection of tibiofemoral joints occurred upon euthanasia (CO^2 exposure and cervical dislocation) at either 3-, 7-, 14-, 56-, 84- or 112-days post-injury, or 0-days for non-surgical baseline controls. All animal procedures were approved by the University of Delaware's Institutional Animal Care and Use Committee (Protocol Number 1252).

Histological Processing and Staining: Following tissue collection, joints were processed for paraffin embedding, sectioning, and histological staining using standard techniques[25]. Briefly, all joints were placed within tissue cassettes at a flexion angle of ~80º, approximating the joint's natural flexed position. Specimens were then fixed in 4% paraformaldehyde for 48-hours at 4ºC, decalcified in 14% EDTA (pH 7.4) over 15-days at 4ºC, and processed for paraffin embedding. Joints were serially cut into 5-µm thick coronal sections and placed on charged slides (two sections/slide). Starting at the front of the joint (anterior), every tenth slide (every ~100-µm) was stained with 1% Safranin-O, 0.02% fast green, and Weigert's iron hematoxylin. From these, a subset of five slides spanning ~500-µm of the joint and centered about the tibial plateau and femoral condyle cartilage contact region were selected for damage analysis (Figure 1A). These slides were labeled (1-5), from the anterior to the posterior level of the joint.

Spatiotemporal Scoring of Width- and Depth-Based Cartilage Damage: Semi-quantitative scoring of cartilage damage was performed across all stages of disease development (3- to 112-days). Three blinded scorers (MAD, MKS, and ATW or RNP) scored the degree of cartilage damage present in each slide using two separate semi-quantitative scoring metrics to evaluate the extent of width- vs. depth-wise cartilage damage. Width-wise damage across the articular surface was assessed (Figure 1D, Table 1) using a modified version of the OARSI scoring system[25]. Depth-wise cartilage damage, relative to the calcified cartilage/subchondral bone interface (Figure 1D, Table 1), was assessed using an adapted version of Chambers' et al.[23] scoring system. For each metric, cartilage damage was assessed on a 0-6 scale. Scores of 0-2 were applied identically within both scoring systems, while scores of 3-6 differed among systems. This allowed for classification of cartilage erosion based on its width-wise extent independent of depth-wise extent, and vice versa. Scoring was performed and aggregated separately for each of

the four compartments of the joint: the medial tibial plateau (MTP), the medial femoral condyle (MFC), the lateral tibial plateau (LTP), and the lateral femoral condyle (LFC) (Figure 1B). Each individual level's scores (anterior [1] to posterior [5]) were aggregated across observers within an individual joint. For overall temporal analysis, all levels' scores were averaged to generate a whole-joint damage score used to calculate group means. For spatial analysis of anterior-to-posterior damage, the average individual specimen score at each level was used to calculate a group mean for each level and time-point.

Quantification of Meniscal Coverage of the Cartilage Surface, Cartilage Damage, and Chondrocyte Cellularity: To establish spatial (medial-to-lateral) and temporal relationships between meniscal extrusion and changes in chondrocyte cellularity and cartilage damage within the medial joint compartment, sections from joints 3- to 84-days post-DMM were stained immunohistochemically (IHC) for type II collagen and DAPI-positive cells (n = 5-mice/group, see Supplemental Methods), and quantified via custom semi-automated image processing. IHC staining was performed on slides adjacent to the Safranin-O sections, and surrounding the center of cartilage contact (levels 2-4). Following staining, overlapping images of the sections were captured at 20x magnification using an epifluorescent microscope (Axio.Observer.Z1, Carl Zeiss) and a digital camera (AxioCam MrC, Zeiss) and combined (tiled) using Zen software (Zeiss). A custom semi-automated MATLAB (MathWorks) algorithm was used to: i) define the MTP region of interest (ROI) in each image, ii) manually trace the articular cartilage (AC), calcified cartilage (CC), and medial meniscus, and iii) count DAPI-positive cells within each ROI (Supplementary Figure 1). Traces were automatically segmented width-wise into four regions (quadrants 1-4; Supplementary Figure 1) and cartilage structural (i.e., AC and CC thickness) and cellular (i.e., number of DAPI-positive cells) parameters were quantified within

each quadrant. Quadrant 1 represents the innermost region of the joint while quadrant 4 was nearest the joint margin. Additionally, the degree of meniscal extrusion was calculated as the extent of cartilage surface covered by the meniscus (length of meniscus covering AC/total AC width; herein referred to as 'meniscal coverage'), and the linear extent of width-wise cartilage surface damage, including fibrillations, clefting, and erosions (length of AC damage/total AC width), were traced and quantified.

Statistical Analysis: All data is presented as mean ± standard deviation. Statistical analyses were performed using GraphPad Prism 6.0. Paired t-tests were used to establish differences in cartilage outcomes between DMM and contralateral joints at each time-point. One-way ANOVAs with Tukey's post-hoc tests were used to determine differences in cartilage outcomes i) between contralateral, sham, and age-matched joints at a given time-point; and ii) over time for either DMM or control joints. Linear regression was performed to identify i) spatial patterns (among levels 1-5) within DMM or contralateral joints, and ii) the relationship between whole-joint depth- versus width-wise damage. Pearson correlation coefficients were calculated to establish the relationships between meniscal extrusion, chondrocyte loss, and cartilage damage. Statistical significance was set at $p<0.05$; however, results exhibiting trends toward significance ($p<0.10$) are indicated.

Results:

Whole-Joint Temporal Changes in Articular Cartilage Structure Post-DMM

Early and progressive changes in AC structure at the whole-joint level were confirmed within the medial compartments of DMM joints (Figure 2 and Supplemental Table 1). Within the MFC, DMM-joints exhibited a trend towards increased whole-joint cartilage damage (i.e., loss of

proteoglycan staining and the presence of fibrillations/clefting) relative to contralateral limbs as early as 7-days (Figure 2A and B), and significant damage accumulation beyond 56-days. In the MTP, similar damage progression was observed in the DMM joints; however, this damage was statistically significant as early as 3-days (score = 0.7; $p<.05$; Figure 2C and D). In both the MFC and MTP of DMM joints, damage appeared to stabilize (scores of ~1-2) between 7- and 56-days before increasing again at 84-days and beyond (scores ≥3; $p<.001$). At 112-days, damage scores highlighted a moderate degree of width- and depth-wise cartilage erosion (~25-50% of the MTP width involved and ~50% of the AC depth; scores = 3.3 and 3.4, respectively). No significant cartilage damage was observed within the lateral compartments of DMM compared to contralateral joints or within contralateral joints compared to sham, age-matched, and non-surgical controls (Supplemental Table 1).

We also investigated whether the use of semi-quantitative scoring of width- or depth-wise erosion resulted in different interpretations of AC damage progression by plotting MFC and MTP width-wise scores against their paired depth-wise scores and performing linear regression (Supplemental Figure 2). Damage scores ≤2 are classified identically in both schemes, and thus exhibit an expected one-to-one relationship (MFC [slope = .98; r^2 = .99] and MTP [slope = 1.0; r^2 = .99]). However, we observed that for scores >2 the slope of the linear regression differed significantly from 1.0 in the MTP (slope = .75; r^2 = .79), indicating a slight, albeit significant preference for higher width-wise damage scores. A slight trend towards significance was observed in scores > 2 in the MFC (slope = .83; r^2 = .86). However, the overall interpretation of damage progression remained similar (Figure 2).

Anterior-to-Posterior Distribution of Cartilage Damage Post-DMM

To determine the anterior-to-posterior progression of cartilage damage within the joint, we investigated the distribution of semi-quantitative histological scores across the medial compartment from level 1 (anterior) to level 5 (posterior) over time. Our qualitative impression of preferential, anteriorly-localized damage (Figure 3) was confirmed by semi-quantitative analysis of damage distribution among Safranin-O-stained sections (Figure 4). In the MFC of DMM joints, no significant spatial preference was observed at any time-point (width-wise Figure 4A; depth-wise Supplementary Figure 3). In contrast, anteriorly-localized damage was observed at later-stage disease (width-wise damage p=0.02 & 0.08 at 84- and 112-days, respectively, Figure 4B; depth-wise Supplementary Figure 3). Combined, these data suggest that DMM-induced cartilage damage initiates early and progresses anteriorly-to-posteriorly within the MTP.

Meniscal Coverage of the Articular Cartilage Surface Post-DMM

Qualitative observations in both Safranin-O and IHC stained sections (Figure 5) reinforced our impressions of a spatial relationship between AC damage in the joint and meniscal extrusion post-DMM. IHC sections (type II collagen) were used to measure the extent of the central MTP (levels 2-4) covered by the medial meniscus. In non-surgical controls and contralateral limbs, ~50% of the MTP was covered by the medial meniscus throughout the study (Figure 6). In contrast, an immediate ~30-40% reduction in meniscal coverage of the MTP was seen at 3- and 7-days (p=0.16 and 0.05, respectively). MTP coverage stabilized at ~20% coverage (60% reduction compared to contralateral joints; p=0.001) by 56-days. As a result of meniscal extrusion, a full quarter of the central contact region of the MTP (and MFC), largely consisting of quadrant 3 [Q3], experienced an acute and persistent change in meniscal coverage. These findings confirmed the outward extrusion of the medial meniscus within the joint post-

DMM, and identified the specific regions of the AC that are exposed to potentially altered contacts and mechanics due to changes in meniscal coverage.

Distribution of Width-Wise MTP Articular Cartilage Damage Post-DMM

To assess the width-wise extent of surface damage and erosions not captured by our semi-quantitative scoring system, we quantitated the linear width-wise damage, which included fibrillations (score of 1), clefting (2), and erosions (≥3), across the MTP surface in our IHC-stained sections. We observed that the extent of damaged surface increased from ~0 to 35% of the MTP cartilage width between 0- and 7-days (Figure 7A), then stabilized at ~35-40% for the remainder of the study. We also observed that the extent of compromised cartilage surface was inversely correlated with the extent of meniscal coverage ($R^2 = .40$ and $p < .001$; Figure 7B) and that the spatial location of this damage was typically centered about newly exposed Q3 of the MTP (data not shown). In the same sections, we measured the average thickness of the AC and CC within each quadrant (Q1-4) to quantify the spatiotemporal progression of cartilage erosion. Interestingly, a statistically significant reduction in AC thickness was only observed within Q3 at 84-days (Supplementary Figure 4). CC thickness was not found to vary appreciably in the present experiment (data not shown). We also qualitatively observed that the linear extent of width-wise damage coincided with an increase in type II collagen staining in both the DMM and contralateral joints (Figure 5). Collagen staining intensity appeared greater at all time-points in DMM-joints, while also appearing to co-localize to AC regions demonstrating a loss of Safranin-O staining, and later overt damage. Taken together, these data suggest that damage accumulated rapidly across the AC, in the form of fibrillations, clefts, and increased type II collagen staining, specifically in MTP regions that lost meniscal coverage due to meniscal extrusion.

Spatiotemporal Changes in Medial Tibial Plateau Chondrocyte Cellularity Post-DMM

Lastly, in analyzing IHC-stained sections we observed alterations in the spatial distributions of chondrocytes (DAPI-positive cells) within the AC post-DMM (Figure 5). As early as 3-days, a significant loss of chondrocytes was seen in Q3 AC of DMM joints' (~60% reduction compared to contralateral joints, p=0.005; Figure 8), which progressed until that quadrant was effectively devoid of chondrocytes by 84-days. In Q1, chondrocyte number remained unchanged, while Q2 and Q4 exhibited less substantial chondrocyte losses post-DMM (Figures 8A). In contralateral joints, no significant changes in chondrocyte number were observed. Furthermore, we observed that the number of AC chondrocytes in quadrants 2, 3, and 4 were linearly correlated to the degree of meniscal coverage (Figure 8B). No significant correlation between meniscal coverage and chondrocyte number was observed in Q1. Chondrocyte numbers in MTP CC remained unaltered (data not shown). Together, this data suggests that chondrocyte loss post-DMM co-localized to AC quadrants that experienced an immediate loss of meniscal coverage (Q3) and prior to subsequently developing extensive cartilage damage (fibrillations, clefts, and erosions) in the same locations.

Discussion:

In the present study, we identified early, localized chondrocyte loss and cartilage damage in the murine DMM model of PTOA using semi-quantitative histological scoring and quantitative analysis of cartilage damage. The findings of immediate cellular, compositional, and structural changes to cartilage highlighted the rapidity of the post-DMM injury response in male C57BL/6 mice and refined the timeline of damage initiation following meniscal destabilization. While our findings were consistent with previous semi-quantitative studies of DMM in the mouse[4–22,26,28], rat[30], and rabbit[29], and with early clinical changes seen in human cartilage following ACL tears[33], we also observed that semi-quantitative cartilage scoring schemes,

whether based upon width- or depth-wise classifications, did not provide a complete picture of the progression of cartilage degeneration. Instead, through implementation of detailed spatial analysis of cartilage damage progression, we uncovered additional aspects of the post-DMM cartilage injury response. Specifically, a strong relationship between meniscal extrusion/coverage and the location/progression of AC cellularity and structural changes.

Under physiological conditions, the meniscus stabilizes the joint and transmits load during articulation[34]. After meniscal detachment from the tibia, either from natural root tears or surgical procedures (like DMM), the meniscus' stabilizing function is lost as wedging effects[34] between the femoral condyle and meniscus causes its extrusion medially into the joint space. As a result of this alteration, several joint-level changes occur, including increased joint laxity and anterior motion[28], and increased tibial plateau contact stresses[10,29]. Clinically, increased meniscal extrusion has been related to increased cartilage damage[35–37]. Our findings in the murine DMM model are consistent with these observations. We observed that DMM-induced meniscal extrusion led to an immediate alteration in meniscal coverage of the MTP AC surface, and the co-localization of cartilage changes (e.g. loss of chondrocytes and proteoglycan content, surface damage, and overt erosions) to the uncovered regions.

Through the detailed spatiotemporal dissection of cartilage damage, the present study provides insight into the anterior-to-posterior and medial-to-lateral progression of cartilage damage post-DMM. While the present analysis demonstrating increased anterior-localized MTP damage was limited to coronal sections spanning the central-cartilage-contact-region of each joint, and may exclude damage more anteriorly or posteriorly, our results were consistent with similar observations made by Glasson et al., in the initial murine DMM study[3]. Analysis of a small set of sagittally-sectioned joints also confirmed our findings across the full MTP, while

also suggesting an increase damage in the MFC anteriorly. This was not evident in the semi-quantitative analysis, potentially due to increased variability within femoral cartilage scoring[25]. Additionally, the sagittal sections from joints 3-days post-DMM demonstrated, similar to the Glasson study[3], no signs of the DMM procedure inducing inadvertent cartilage damage. Interpreting these results in light of established joint-level biomechanical changes[10,28,29] supports the hypothesis that DMM-mediated meniscal extrusion causes altered anterior-to-posterior loading of the knee joint and subsequent anteriorly-to-centrally localized cartilage damage.

A distinct and informative pattern of medial-to-lateral damage progression in the medial joint post-DMM was also observed. Damage across the width of the MTP surface accumulated rapidly and then stabilized, resulting in the presence of extensive fibrillation and clefting to ~20-40% of the MTP surface by 7-days, with this damage being localized to MTP regions experiencing alterations in meniscal coverage due to meniscal extrusion. Interestingly, as time progressed (84+-days) cartilage erosions and a decrease in AC thickness also co-localized to the same MTP regions experiencing alterations in meniscal coverage. Similar findings were observed for the MFC (data not shown). The highly focal nature of this damage highlights the important role of meniscal extrusion/coverage in establishing the location of damage initiation and progression in the DMM model. While this study was not designed to establish the cause of this focal damage progression, several mechanisms could be involved including: i) alterations in cartilage-on-cartilage and cartilage-on-meniscus contact mechanics[28,29] following extrusion, ii) differences in the mechanical properties of cartilage tissues previously covered by the meniscus [38–40], and/or iii) changes in the accessibility of inflammatory[41] and pro-catabolic mediators to the local cartilage regions following injury. Determining if these, or other, mechanisms are involved in the observed phenomena requires further investigation. The apparent stabilization of AC

surface fibrillation and clefting between 7- and 56-days post-DMM was interesting, but was consistent with previous studies[4]. This may reflect a natural ability of the cartilage extracellular matrix to withstand alterations in the tissue's mechanical environment and even loss of resident chondrocytes, temporarily, before developing into larger erosions at later disease stages.

A potentially more significant finding with regards to understanding PTOA initiation was the identification of a striking, immediate, and highly focal loss of chondrocytes within the AC of injured joints post-DMM. As early as 3-days, a drastic decrease in chondrocyte number was observed within the regions of the MTP that experienced changes in meniscal coverage (Q3). Over time, chondrocyte number continued to decrease in DMM joints compared to their contralateral joints until there was a complete loss of cells in Q3, and a moderate loss of chondrocytes in adjacent quadrants. Given the critical role that chondrocytes play in the maintenance, repair, and regeneration of articular cartilage[42], this rapid and focal loss of chondrocytes may constitute the precipitating biological event leading to the initiation and progression of PTOA. This idea is supported by two observations: i) that cartilage erosions predominately localize to areas of earlier chondrocyte loss within and surrounding the 'uncovered' quadrant (Q3), and ii) that the innermost MTP quadrant (Q1) appeared more resistant to both chondrocyte loss and cartilage damage.

While the rapid and localized loss of chondrocytes within the AC of DMM joints in the present study was remarkable, the biological mechanisms underlying this pattern of cell loss remains unknown. Numerous studies implicate chondrocyte necrosis and apoptosis in the initiation and progression of cartilage degeneration following severe, acute cartilage injury in vitro[41,43], and in murine DMM models of PTOA[4,6,24,26,32]. In a non-invasive murine ACL transection study, co-localization of chondrocyte apoptosis to specific regions of injurious load

application was identified 5-days post-injury[31] and a loss of DAPI-positive cells was observed at 14-days, a finding consistent with the present study. The early and rapid loss of chondrocytes in our study also indicate that significant changes in chondrocyte health occur very quickly, prior to 3-days, following DMM-injury. In this regard, a recent study by Burleigh et al.[11] identified changes in gene expressions within murine cartilage as early as 6 hours post-DMM, supporting rapid changes in chondrocyte health/metabolism. Further studies are required to establish: i) whether the observed loss of chondrocytes in DMM-joints is attributable to apoptotic or necrotic events; ii) when, relative to the timing of injury, such critical biological changes are initiated; and iii) the molecular and cellular mechanisms that precipitate these changes.

Of important note is that this present study focused on the role of DMM-induced meniscal extrusion on the spatiotemporal of cartilage changes in male C57BL/6 mice due to the pervasive use of the DMM model[4–22,28,44,45] and the increased susceptibility for these mice to develop cartilage damage in this model[27]. Whether similar outcomes would be observable in female C57BL/6 mice[27] or in other mouse strains[3], species[29,30], and destabilizing injury models[31,46,47] requires further investigation. However, given the similarities in the progression of cartilage damage among murine DMM and other injury models, we suspect that the observed relationships may be a general feature of PTOA initiation and progression.

Lastly, the present findings have several implications regarding the study of PTOA prevention and treatment in the DMM model and translational studies. The focal population of cells identified here represent an ideal target upon which to investigate the chondroprotective effects of various pre-clinical therapies, including joint unloading/rehabilitation[11] and pharmacological interventions[12,14,17,22]. However, it appears that such interventions may need to be initiated immediately/shortly following injury to have the greatest anti-osteoarthritic potential

an observation, which may explain the equivocal findings of chondroprotective drugs within clinical trials[48]. Alternatively, the presence of an apparent plateau in the progression of cartilage damage, between ~7-56-days post-DMM, supports the possibility of the DMM-model as a platform to test alternative treatment targets based on cartilage regeneration[49].

In conclusion, the approaches described here present a benchmark for the detailed study of cartilage damage progression within murine models of surgery-/injury-induced PTOA while providing detailed analyses of the spatiotemporal progression and relationships between cartilage damage, changes in chondrocyte cellularity, and meniscal extrusion within the murine DMM PTOA model from early through late stage disease. This study also provides a comprehensive baseline for ongoing assessment of the cellular and molecular pathoetiology of PTOA, as well as the study of its prevention and treatment.

Acknowledgements

The authors would like to thank Mr. Frank Warren and Dr. Gwen Talham, DVM for oversight of animal care, Brianna Gietter, Olivia Laxton, and Fiona Flowerhill for assistance in preparing histological samples, and Brian Graham for assisting with MATLAB programming. This study was supported by a grant from the US DOD CDMRP PRMRP PR120788P1.

Conflict of Interest Statement:

The authors have no conflicts of interest to report.

References:

1. Lohmander LS, Englund PM, Dahl LL, Roos EM. 2007. The long-term consequence of anterior cruciate ligament and meniscus injuries: osteoarthritis. Am. J. Sports Med.

35:1756–1769.

2. Anderson DD, Chubinskaya S, Guilak F, et al. 2011. Post-traumatic osteoarthritis: Improved understanding and opportunities for early intervention. J. Orthop. Res. 29(June):802–809.

3. Glasson SS, Blanchet TJ, Morris E a. 2007. The surgical destabilization of the medial meniscus (DMM) model of osteoarthritis in the 129/SvEv mouse. Osteoarthr. Cartil. 15:1061–1069.

4. Leahy A a., Esfahani S a., Foote AT, et al. 2015. Analysis of the Trajectory of Osteoarthritis Development in a Mouse Model by Serial Near-Infrared Fluorescence Imaging of Matrix Metalloproteinase Activities. Arthritis Rheumatol. 67(2):442–453.

5. Kim BJ, Choi BH, Jin LH, et al. 2013. Comparison between subchondral bone change and cartilage degeneration in collagenase-and DMM-induced osteoarthritis (OA) models in mice. Tissue Eng. Regen. Med. 10(4):211–217.

6. Loeser RF, Olex AL, McNulty M a., et al. 2013. Disease Progression and Phasic Changes in Gene Expression in a Mouse Model of Osteoarthritis. PLoS One 8(1).

7. Kim BJ, Kim DW, Kim SH, et al. 2013. Establishment of a reliable and reproducible murine osteoarthritis model. Osteoarthr. Cartil. 21(12):2013–2020.

8. Gardiner MD, Vincent TL, Driscoll C, et al. 2015. Transcriptional analysis of micro-dissected articular cartilage in post-traumatic murine osteoarthritis. Osteoarthr. Cartil. 23(4):616–628.

9. Inglis JJ, McNamee KE, Chia SL, et al. 2008. Regulation of pain sensitivity in

experimental osteoarthritis by the endogenous peripheral opioid system. Arthritis Rheum. 58(10):3110–3119.

10. Das Neves Borges P, Forte a. E, Vincent TL, et al. 2014. Rapid, automated imaging of mouse articular cartilage by microCT for early detection of osteoarthritis and finite element modelling of joint mechanics. Osteoarthr. Cartil. 22(10):1419–1428.

11. Burleigh A, Chanalaris A, Gardiner MD, et al. 2012. Joint immobilization prevents murine osteoarthritis and reveals the highly mechanosensitive nature of protease expression in vivo. Arthritis Rheum. 64(7):2278–2288.

12. Takayama K, Kawakami Y, Kobayashi M, et al. 2014. Local intra-articular injection of rapamycin delays articular cartilage degeneration in a murine model of osteoarthritis. Arthritis Res. Ther. 16(6):1–10.

13. Botter SM, Glasson SS, Hopkins B, et al. 2009. ADAMTS5-/- mice have less subchondral bone changes after induction of osteoarthritis through surgical instability: implications for a link between cartilage and subchondral bone changes. Osteoarthr. Cartil. 17(5):636–645.

14. Muramatsu Y, Sasho T, Saito M, et al. 2014. Preventive effects of hyaluronan from deterioration of gait parameters in surgically induced mice osteoarthritic knee model. Osteoarthr. Cartil. 22(6):831–835.

15. Xu L, Servais J, Polur I, et al. 2010. Attenuation of osteoarthritis progression by reduction of discoidin domain receptor 2 in mice. Arthritis Rheum. 62(9):2736–2744.

16. Van Lent PLEM, Blom AB, Schelbergen RFP, et al. 2012. Active involvement of alarmins S100A8 and S100A9 in the regulation of synovial activation and joint

434 destruction during mouse and human osteoarthritis. Arthritis Rheum. 64(5):1466–1476.

435 17. Akagi R, Sasho T, Saito M, et al. 2014. Effective knock down of matrix
436 metalloproteinase-13 by an intra-articular injection of small interfering RNA (siRNA) in a
437 murine surgically-induced osteoarthritis model. J. Orthop. Res. 32(9):1175–1180.

438 18. Glasson SS, Askew R, Sheppard B, et al. 2004. Characterization of and osteoarthritis
439 susceptibility in ADAMTS-4-knockout mice. Arthritis Rheum. 50(8):2547–2558.

440 19. Glasson SS, Askew R, Sheppard B, et al. 2005. Deletion of active ADAMTS5 prevents
441 cartilage degradation in a murine model of osteoarthritis. Nature 434(7033):644–648.

442 20. Li W, Cai L, Zhang Y, et al. 2015. Intra-articular resveratrol injection prevents
443 osteoarthritis progression in a mouse model by activating SIRT1 and thereby silencing
444 HIF-2?? J. Orthop. Res. 1(July):1061–1070.

445 21. Pan J, Wang B, Li W, et al. 2012. Elevated cross-talk between subchondral bone and
446 cartilage in osteoarthritic joints. Bone 51(2):212–217.

447 22. Sophocleous a., Börjesson a. E, Salter DM, Ralston SH. 2015. The type 2 cannabinoid
448 receptor regulates susceptibility to osteoarthritis in mice. Osteoarthr. Cartil. :1–9.

449 23. Chambers MG, Bayliss MT, Mason RM. 1997. Chondrocyte cytokine and growth factor
450 expression in murine osteoarthritis. Osteoarthr. Cartil. 5:301–308.

451 24. McNulty M a., Loeser RF, Davey C, et al. 2011. A Comprehensive Histological
452 Assessment of Osteoarthritis Lesions in Mice. Cartilage 2(4):354–363.

453 25. Glasson SS, Chambers MG, Berg WB van den, Little CB. 2010. The OARSI
454 histopathology initiative - recommendations for histological assessments of osteoarthritis

in the mouse. In: Osteoarthritis and cartilage / OARS, Osteoarthritis Research Society. Pfizer, Tissue Repair, 200 CambridgePark Drive, Cambridge, MA 02140, USA. ssglasson@gmail.com: Elsevier Ltd; p S17–23.

26. Little CB, Barai A, Burkhardt D, et al. 2009. Matrix metalloproteinase 13-deficient mice are resistant to osteoarthritic cartilage erosion but not chondrocyte hypertrophy or osteophyte development. Arthritis Rheum. 60(12):3723–3733.

27. Ma HL, Blanchet TJ, Peluso D, et al. 2007. Osteoarthritis severity is sex dependent in a surgical mouse model. Osteoarthr. Cartil. 15(6):695–700.

28. Moodie JP, Stok KS, M??ller R, et al. 2011. Multimodal imaging demonstrates concomitant changes in bone and cartilage after destabilisation of the medial meniscus and increased joint laxity. Osteoarthr. Cartil. 19(2):163–170.

29. Arunakul M, Tochigi Y, Goetz JE, et al. 2013. Replication of chronic abnormal cartilage loading by medial meniscus destabilization for modeling osteoarthritis in the rabbit knee in vivo. J. Orthop. Res. 31(10):1555–1560.

30. Iijima H, Aoyama T, Ito a., et al. 2014. Destabilization of the medial meniscus leads to subchondral bone defects and site-specific cartilage degeneration in an experimental rat model. Osteoarthr. Cartil. 22(7):1036–1043.

31. Wu P, Holguin N, Silva MJ, et al. 2014. Early response of mouse joint tissue to noninvasive knee injury suggests treatment targets. Arthritis Rheumatol. 66(5):1256–1265.

32. McNulty MA, Loeser RF, Davey C, et al. 2012. Histopathology of naturally occurring and

surgically induced osteoarthritis in mice. Osteoarthr. Cartil. 20(8):949–956.

33. Nelson F, Billinghurst RC, Pidoux RT, et al. 2006. Early post-traumatic osteoarthritis-like changes in human articular cartilage following rupture of the anterior cruciate ligament. Osteoarthr. Cartil. 14:114–119.

34. Kawamura S, Lotito K, Rodeo S a. 2003. Biomechanics and healing response of the meniscus. Oper. Tech. Sports Med. 11(2):68–76.

35. Lerer DB, Umans HR, Xu MX, Jones MH. 2004. The role of meniscal root pathology and radial meniscal tear in medial meniscal extrusion. Skeletal Radiol. 33(10):569–574.

36. Hunter DJ, Zhang YQ, Niu JB, et al. 2006. The association of meniscal pathologic changes with cartilage loss in symptomatic knee osteoarthritis. Arthritis Rheum. 54(3):795–801.

37. Bin S Il, Jeong TW, Kim SJ, Lee DH. 2016. A new arthroscopic classification of degenerative medial meniscus root tear that correlates with meniscus extrusion on magnetic resonance imaging. Knee 23(2):246–250.

38. Thambyah A, Nather A, Goh J. 2006. Mechanical properties of articular cartilage covered by the meniscus. Osteoarthr. Cartil. 14(6):580–588.

39. Iijima H, Aoyama T, Ito A, et al. 2014. Immature articular cartilage and subchondral bone covered by menisci are potentially susceptive to mechanical load. BMC Musculoskelet. Disord. 15(1):101.

40. Moore AC, Burris DL. 2015. Tribological and material properties for cartilage of and throughout the bovine stifle: Support for the altered joint kinematics hypothesis of

497 osteoarthritis. Osteoarthr. Cartil. 23(1):161–169.

498 41. Stolberg-Stolberg JA, Furman BD, William Garrigues N, et al. 2013. Effects of cartilage
499 impact with and without fracture on chondrocyte viability and the release of inflammatory
500 markers. J. Orthop. Res. 31(8):1283–1292.

501 42. Sophia Fox a. J, Bedi A, Rodeo S a. 2009. The Basic Science of Articular Cartilage:
502 Structure, Composition, and Function. Sport. Heal. A Multidiscip. Approach 1(6):461–
503 468.

504 43. Chen CT, Burton-Wurster N, Borden C, et al. 2001. Chondrocyte necrosis and apoptosis
505 in impact damaged articular cartilage. J. Orthop. Res. 19(4):703–711.

506 44. Miller RE, Tran PB, Das R, et al. 2012. CCR2 chemokine receptor signaling mediates
507 pain in experimental osteoarthritis. Pnas 109(50):2–7.

508 45. Malfait AM, Ritchie J, Gil AS, et al. 2010. ADAMTS-5 deficient mice do not develop
509 mechanical allodynia associated with osteoarthritis following medial meniscal
510 destabilization. Osteoarthr. Cartil. 18(4):572–580.

511 46. Kamekura S, Hoshi K, Shimoaka T, et al. 2005. Osteoarthritis development in novel
512 experimental mouse models induced by knee joint instability. Osteoarthr. Cartil. 13:632–
513 641.

514 47. Furman BD, Strand J, Hembree WC, et al. 2007. Joint degeneration following closed
515 intraarticular fracture in the mouse knee: A model of posttraumatic arthritis. J. Orthop.
516 Res. 25(5):578–592.

517 48. Felson DT, Kim YJ. 2007. The futility of current approaches to chondroprotection.

518 Arthritis Rheum. 56(5):1378–1383.

519 49. Hunziker EB. 2002. Articular cartilage repair: Basic science and clinical progress. A
520 review of the current status and prospects. Osteoarthr. Cartil. 10(2001):432–463.

521

522

Table 1. Description of the semi-quantitative width- and depth-based histological scoring systems utilized in the present study.

Score	Width-Based	Depth-Based
0	Normal	
0.5	Loss of Safranin-O without structural changes*	
1	Fibrillations/discontinuities and/or roughened superficial surface*	
2	Erosion to the layer immediately below the superficial layer and some loss of surface lamina*	
3	Erosion[#] extending <25% of AC width	Erosion[#] extending for <25% of total cartilage depth[‡]
4	Erosion[#] extending 25-50% of AC width	Erosion[#] extending for 25-50% of total cartilage depth[‡]
5	Erosion[#] extending 50-75% of AC width	Erosion[#] extending for 50-75% of total cartilage depth[‡]
6	Erosion[#] extending >75% of AC width	Erosion[#] extending for >75% of total cartilage depth[‡]

[*] indicates damage can extend across any percentage (%) of the articular cartilage surface width

[#] indicates erosion must extend beyond the layer immediately below the superficial layer/lamina

[‡] indicates depth measured relative to total cartilage (AC + CC) thickness

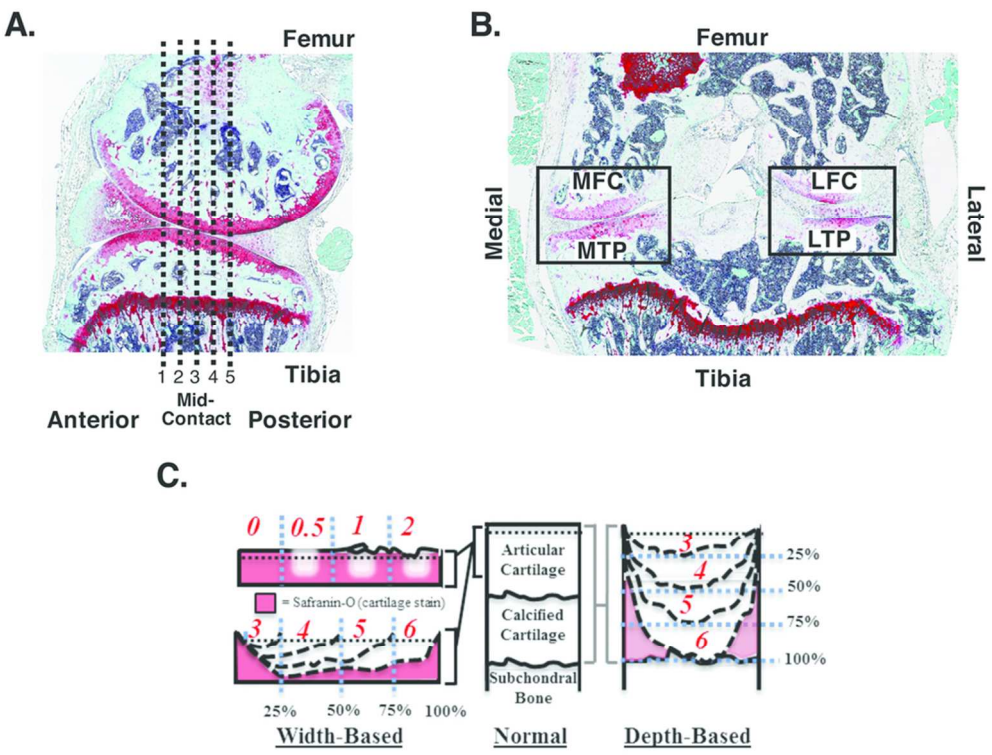

Figure 1. Histological analysis of cartilage structural damage. Safranin-O/fast green stained sections from: (A.) a representative sagittal section of a joint demonstrating the region of interest, and the approximate position of the coronal slides (anterior - level 1 to posterior - level 5) selected for experimental analysis, and (B.) a representative coronal section used for histological analysis. Black boxes indicate the separate compartments and regions of the joint that were analyzed via semi-quantitative histological scoring at higher resolution - the medial femoral condyle (MFC), medial tibial plateau (MTP), lateral femoral condyle (LFC), lateral tibial plateau (LTP). (C.) Schematic of the width- and depth-based semi-quantitative histological scoring systems utilized in the study. Damage was scored on a 0-6 scale; values of 0-2 are identical in both scoring systems and only extend to the layer immediately below the superficial layer (dotted black line). Scores of 3 and higher differ between systems, allowing for both width- and depth-based erosions to be accounted for independently. A complete description of the scoring system can be found in Table 1.

85x64mm (300 x 300 DPI)

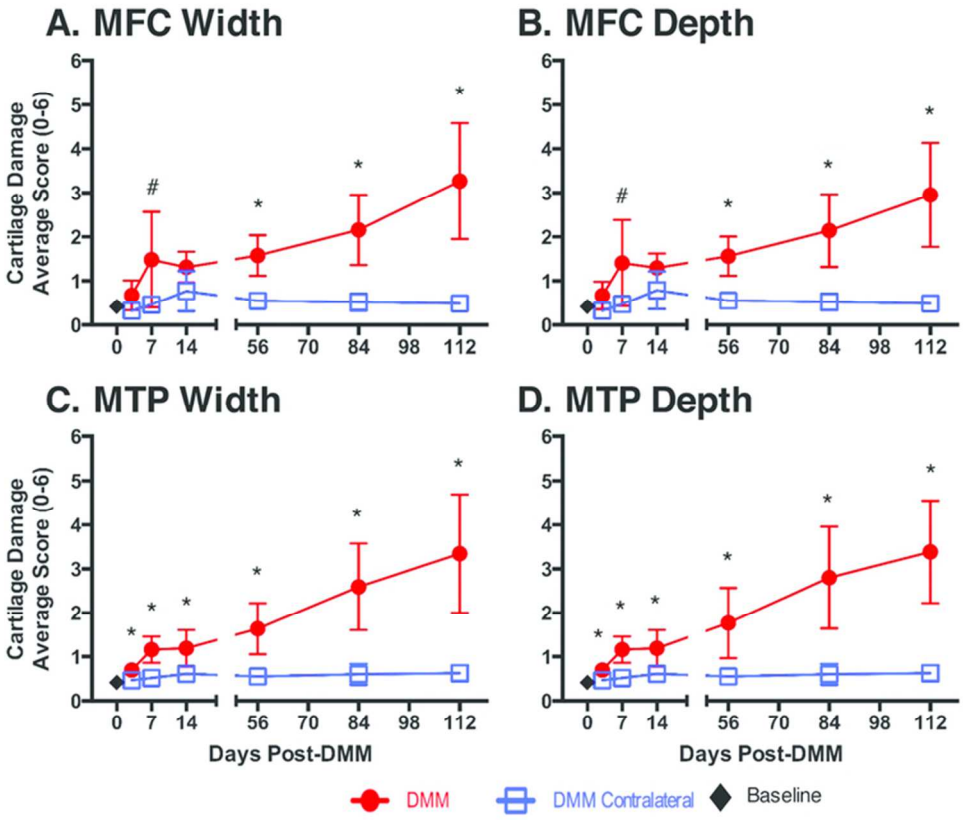

Figure 2. Temporal progression of whole-joint level cartilage damage in the medial femoral condyle (A. and B.) and medial tibial plateau (C. and D.) of murine knee joints post-DMM. Semi-quantitative histological scoring demonstrated the rapid accumulation of significant overall proteoglycan loss and surface fibrillations [scores = .5-1] as early as 3-days in the MTP of DMM joints, which then stabilized between 7- and 56-days as surface fibrillations and clefts [scores = 1-2], before progressing into larger width-wise (C.) and depth-wise (D.) erosions [scores ≥3] at 84-days and beyond. Similar trends were observed for the MFC (A. and B.); however, they only reached statistical significance at 56-days and onward. Results are presented as mean ± STD (n = 5-10/time point/group) where * = $p<0.05$, # = $p<0.10$ (trend) for paired t-test between DMM and DMM contralateral.

66x55mm (300 x 300 DPI)

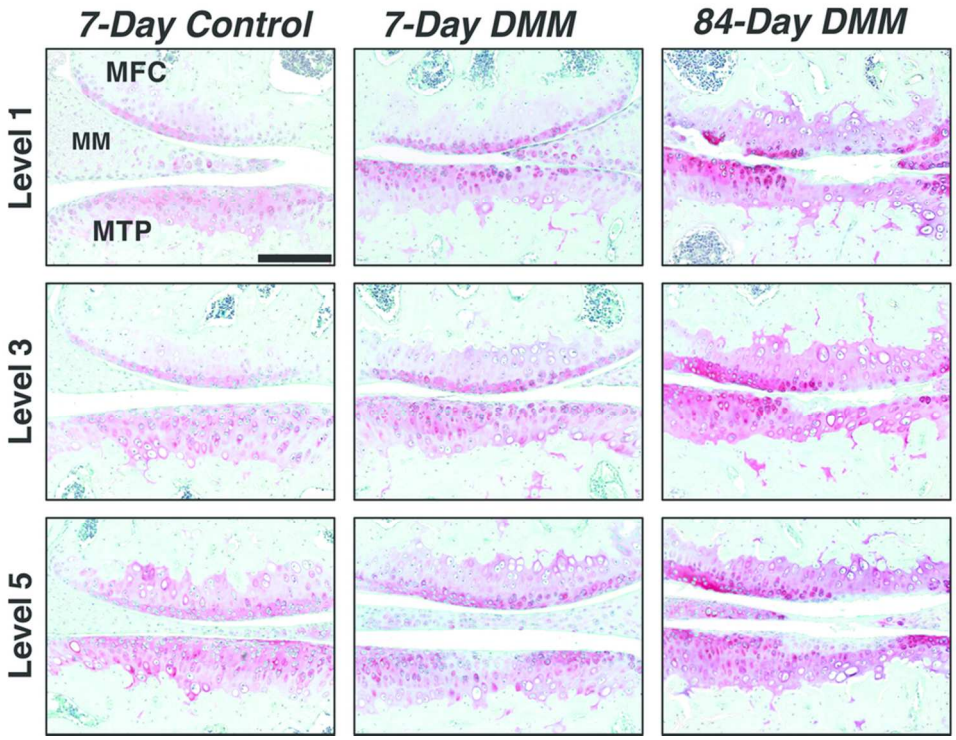

Figure 3. Spatiotemporal progression of cartilage damage in the medial compartment of the knee joint post-DMM. Safranin-O stained sections highlight the changes in the medial meniscus (MM) location and the distribution of cartilage damage from the anterior (level 1), through mid-contact (level 3) and posterior (level 5) levels of DMM and contralateral (control) joints following DMM-injury. Anteriorly-localized cartilage damage was observed in the medial tibial plateau (MTP) of DMM-joints at 84-days and beyond. In contrast, no preference for anterior-to-posterior damage localization was observed for medial femoral condyle (MFC) cartilage. No damage was observed in controls. All images were acquired at 20x magnification, scale bar (200-um, A1) applies to all images.

85x63mm (300 x 300 DPI)

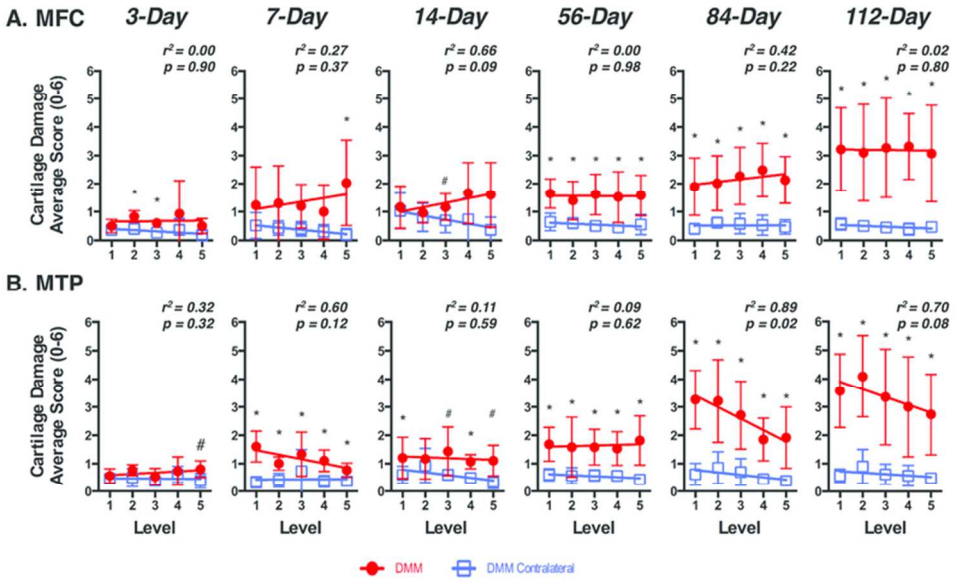

Figure 4. Anterior-to-posterior distribution of width-wise cartilage damage within the medial compartment of DMM joints. To confirm our qualitative observations, the distribution of semi-quantitative width-wise cartilage damage scores in the medial femoral condyle (MFC; A.) and tibial plateau (MTP; B.), from anterior (level 1) to posterior (level 5) aspects of the central cartilage contact of the joint, were evaluated overtime. No specific pattern of damage localization was observed in the MFC of DMM joints. In contrast, the MTP demonstrated significantly increased damage anteriorly compared to posteriorly at late time-points (84- and 112-days) following DMM. Damage across the MFC and MTP of contralateral (control) joints was minimal, and exhibited no spatial patterning. Results are presented as mean ± STD (n = 5-10/time point/group) where * = $p<0.05$ and # = $p<0.10$ (trend) for paired t-test between DMM and contralateral joints at a given level. Linear regression r2- and p-values are shown for DMM joints only.

70x41mm (300 x 300 DPI)

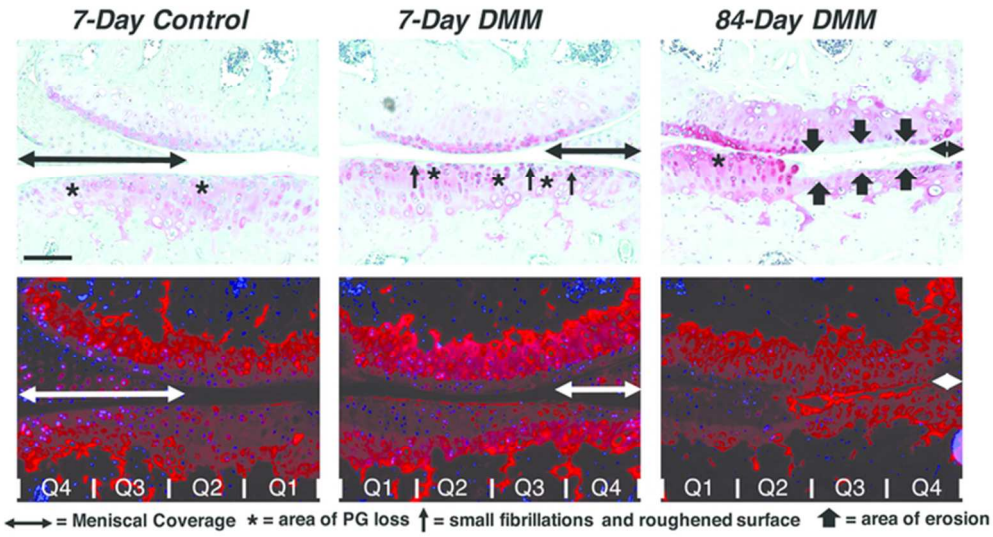

Figure 5. Histological and immunohistochemical representation of the medial-to-lateral distribution of cartilage damage, meniscal coverage, and chondrocyte presence post-DMM. Adjacent histological (Safranin-O/fast green [upper panel]) and immunohistochemical (type II collagen and DAPI [lower pane]) images at 7- and 84-days post-DMM. Qualitatively, a distinct loss of proteoglycan staining, loss of chondrocytes, and increased type II collagen staining was observed to co-localize to MTP cartilage regions that experienced a loss of meniscal coverage at 7- and 84-days (Q3). All sections depict images take from anterior-posterior level 2 (anterior-to-mid-contact) and acquired at 20x magnification, scale bar (100-μm, A1) applies to all images.
61x33mm (300 x 300 DPI)

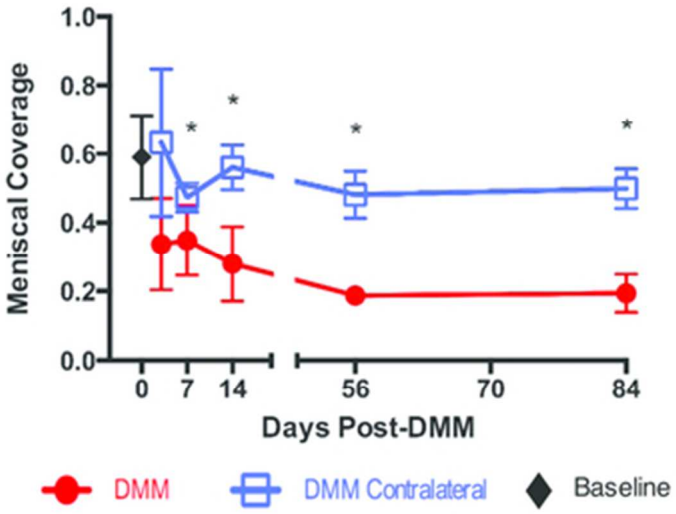

Figure 6. Quantification of the fraction of cartilage surface covered by the medial meniscus (meniscal coverage) post-DMM. Fraction of meniscal coverage was defined from the MTP joint margin towards the innermost regions of the joint. In DMM joints, the MTP experienced a significant loss of meniscal coverage compared to contralateral joints as early as 7-days. This resulted in ~20-40% coverage that stabilized with time. Results are presented as mean ± STD (n = 5/time point/group) where * = $p<0.05$ for paired t-test between DMM and contralateral joints.
30x22mm (300 x 300 DPI)

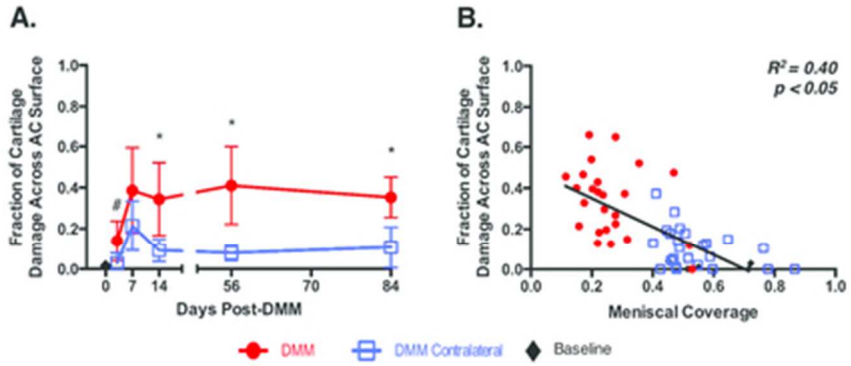

Figure 7. Quantification of the width-wise extent of articular cartilage damage across the MTP post-DMM and its relationship to meniscal coverage. The normalized extent of width-wise cartilage damage across the medial tibial plateau's surface, represented by histological scores of 1 and greater, was quantified. In the DMM joints, a trend towards significantly increased width-wise damage, compared to contralateral joints, was seen as early as 3-days post-DMM (A.). Following this initial accumulation of damage, the extent of damage stabilized at ~35-40% involvement of the MTP width throughout the remainder of the study. The extent of width-wise cartilage damage was inversely related to degree of meniscal coverage (B.); decreased meniscal coverage was accompanied by increased surface damage. Results are presented as mean ± STD (n = 5), where * = $p<0.05$ and # = $p<0.10$ (trend) for paired t-test between DMM and contralateral joints. Pearson correlation coefficients (R2)- and p-values were calculated with DMM, contralateral, and baseline data points included.

36x15mm (300 x 300 DPI)

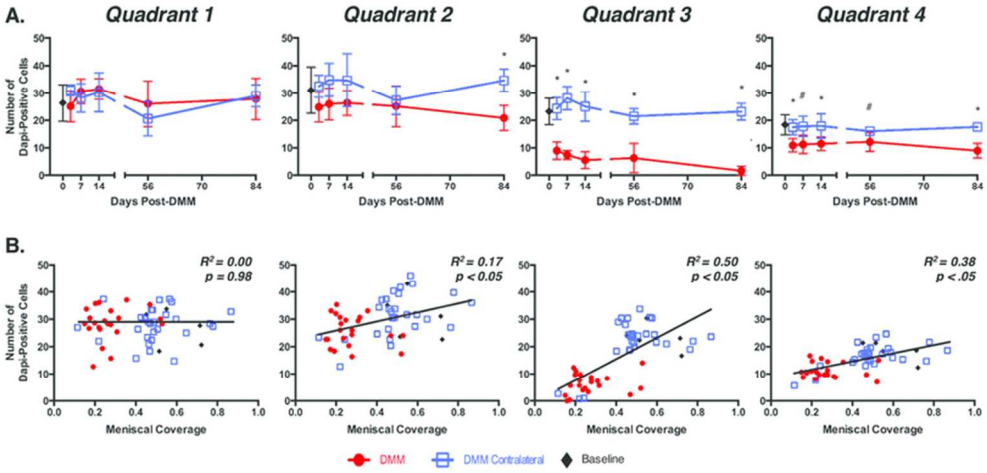

Figure 8. Spatiotemporal quantification of chondrocyte presence within the medial tibial plateau of articular cartilage post-DMM and their relationship to meniscal coverage. The medial tibial plateau experienced a significant loss of chondrocyte number (identified via DAPI-positive staining) that was specifically localized to the MTP quadrants that experienced alterations in medial meniscus coverage following DMM. Quadrants 3 and 4 experienced significant chondrocyte loss as early as 3-days post-DMM, significant chondrocyte loss in quadrant 2 was only seen only at 84-days. No significant changes in chondrocyte number were observed in quadrant 1. In quadrants that experienced a loss of chondrocyte number following DMM, chondrocyte numbers were correlated with meniscal coverage (B.). Results are presented as mean ± STD (n = 5/time point/group) where * = $p<0.05$ and # = $p<0.1$ (trend) for paired t-test between DMM and DMM contralateral. Pearson correlation coefficients (R2)- and p-values were calculated with DMM, contralateral, and baseline data points included.
69x33mm (300 x 300 DPI)

Supplementary Methods:

Immunohistochemical Staining: Sections from DMM and contralateral (control) joints were stained immunohistochemically for type II collagen and the presence of cells (DAPI counterstain for nuclei). Type II collagen was used as a structural indicator to assist in distinguishing between the articular and calcified cartilages within each section and DAPI counterstain was used to differentiate the presence of chondrocytes in each tissue. Briefly, antigen retrieval was performed on the sections using pepsin (0.4% w/v; Sigma) in 0.01N hydrochloric acid for 15 minutes at 37°C. Sections were then blocked with 5% normal donkey serum (Sigma) in phosphate-buffered saline with 0.1% Tween-20 (Fisher Scientific) for one-hour at room temperature (RT), and incubated with a rabbit anti-mouse type II collagen primary antibody (1:200 dilution, ThermoFisher) overnight at 4°C. Sections were then incubated with an AlexaFluor-555 donkey anti-rabbit secondary antibody (1:400, ThermoFisher) for 1 hour at RT in the dark, treated with 0.1% w/v Sudan black (FisherBioReagents™) in 70% ethanol for 30 minutes at RT to reduce autofluorescence, and then mounted with a DAPI-containing mounting medium (ThermoFisher) for the detection of cell nuclei. Fluorescent images of the collagen type II and DAPI stained sections were obtained within 72-hours of completing the immunohistochemical staining procedure to limit fluorescent signal loss.

Supplemental Table 1: Temporal quantification of cartilage damage scoring in DMM, Contralateral, Sham and Age-Matched Joints

	Medial Femoral Condyle (Width-Wise Score)				Lateral Femoral Condyle (Width-Wise Score)			
Days Post-Surgery	DMM	Contralateral	Sham	Age-Matched ‡	DMM	DMM Contralateral	Sham	Age-Matched ‡
3	0.67 ± 0.34	0.33+0.07	0.47 ± 0.20	0.42 ± 0.14	0.55 ± 0.14	0.65 ± 0.28	0.47 ± 0.15	0.39 ± 0.18
7	1.48 ± 1.09	0.46 ± 0.14	0.52 ± 0.11	"	0.71 ± 0.30	0.51 ± 0.27	0.70 ± 0.17	"
14	1.31 ± 0.35	0.77 ± 0.46	0.51 ± 0.08	"	0.63 ± 0.14	0.69 ± 0.36	0.44 ± 0.19	"
56	1.58 ± 0.46***	0.55 ± 0.12	0.41 ± 0.08	0.49 ± 0.27	0.66 ± 0.30	0.70 ± 0.24	0.50 ± 0.05	0.55 ± 0.34
84	2.16 ± 0.80****	0.52 ± 0.19	0.56 ± 0.22	0.47 ± 0.06	0.81 ± 0.35	0.71 ± 0.21	0.83 ± 0.20	0.67 ± 0.19
112	3.27 ± 1.32****	0.49 ± 0.07	0.38 ± 0.02	0.40 ± 0.14	1.34 ± 0.49	1.20 ± 0.46	0.73 ± 0.15	1.16 ± 0.65

	Medial Femoral Condyle (Depth-Wise Score)				Lateral Femoral Condyle (Depth-Wise Score)			
Days Post-Surgery	DMM	DMM Contralateral	Sham	Age-Matched ‡	DMM	DMM Contralateral	Sham	Age-Matched ‡
3	0.67 ± 0.32	0.32 ± 0.07	0.47 ± 0.20	0.42 ± 0.14	0.55 ± 0.14	0.65 ± 0.28	0.47 ± 0.15	0.39 ± 0.18
7	1.41 ± 0.98	0.47 ± 0.13	0.52 ± 0.11	"	0.71 ± 0.30	0.53 ± 0.32	0.70 ± 0.17	"
14	1.30 ± 0.33	0.79 ± 0.43	0.51 ± 0.08	"	0.63 ± 0.14	0.68 ± 0.35	0.44 ± 0.19	"
56	1.57 ± 0.45***	0.55 ± 0.12	0.41 ± 0.08	0.49 ± 0.27	0.64 ± 0.25	0.69 ± 0.21	0.43 ± 0.12	0.55 ± 0.34
84	2.14 ± 0.83****	0.52 ± 0.19	0.56 ± 0.22	0.47 ± 0.06	0.79 ± 0.31	0.71 ± 0.21	0.83 ± 0.20	0.67 ± 0.19
112	2.95 ± 1.18***	0.49 ± 0.08	0.38 ± 0.02	0.41 ± 0.15	1.38 ± 0.55	1.18 ± 0.43	0.73 ± 0.15	1.04 ± 0.51

	Medial Tibia Plateau (Width-Wise Score)				Lateral Tibia Plateau (Width-Wise Score)			
Days Post-Surgery	DMM	DMM Contralateral	Sham	Age-Matched ‡	DMM	DMM Contralateral	Sham	Age-Matched ‡
3	0.70 ± 0.16*	0.47 ± 0.06S	0.73 ± 0.03C,AM	0.42 ± 0.18S	0.70 ± 0.13	0.69 ± 0.19	0.83 ± 0.22	0.51 ± 0.24
7	1.16 ± 0.30*	0.52 ± 0.14	0.59 ± 0.05	"	0.88 ± 0.29	0.77 ± 0.25	0.92 ± 0.21	"
14	1.19 ± 0.42*	0.61 ± 0.16	0.65 ± 0.06	"	0.78 ± 0.20	0.75 ± 0.16	0.57 ± 0.04	"
56	1.64 ± 0.58***	0.55 ± 0.10	0.63 ± 0.17	0.56 ± 0.31	0.93 ± 0.22	0.76 ± 0.23	0.77 ± 0.12	0.68 ± 0.26
84	2.59 ± 0.98****	0.60 ± 0.24	0.61 ± 0.15	0.63 ± 0.15	0.98 ± 0.34	1.01 ± 0.34	1.10 ± 0.31	0.80 ± 0.11
112	3.33 ± 1.35****	0.63 ± 0.18	0.86 ± 0.01	0.74 ± 0.37	1.07 ± 0.34	1.03 ± 0.37	0.96 ± 0.12	0.74 ± 0.21

	Medial Tibia Plateau (Depth-Wise Score)				Lateral Tibia Plateau (Depth-Wise Score)			
Days Post-Surgery	DMM	DMM Contralateral	Sham	Age-Matched ‡	DMM	DMM Contralateral	Sham	Age-Matched ‡
3	0.70 ± 0.16*	0.47 ± 0.06S	0.73 ± 0.03C,AM	0.42 ± 0.18S	0.70 ± 0.13	0.69 ± 0.19	0.83 ± 0.22	0.51 ± 0.24
7	1.16 ± 0.30*	0.52 ± 0.14	0.59 ± 0.05	"	0.88 ± 0.29	0.73 ± 0.23	0.92 ± 0.21	"
14	1.19 ± 0.42*	0.61 ± 0.16	0.65 ± 0.06	"	0.78 ± 0.20	0.75 ± 0.16	0.58 ± 0.04	"
56	1.77 ± 0.80***	0.55 ± 0.10	0.63 ± 0.17	0.56 ± 0.31	0.93 ± 0.22	0.76 ± 0.23	0.77 ± 0.12	0.68 ± 0.26
84	2.80 ± 1.16****	0.60 ± 0.24	0.61 ± 0.15	0.63 ± 0.15	0.97 ± 0.33	1.00 ± 0.32	1.12 ± 0.33	0.80 ± 0.11
112	3.39 ± 1.17****	0.63 ± 0.18	0.86 ± 0.01	0.74 ± 0.37	1.10 ± 0.36	1.03 ± 0.40	0.96 ± 0.12	0.72 ± 0.21

* = Significantly different from respective contralateral joint, $p<0.05$; ** = $p<0.01$; *** = $p<0.001$; **** = $p<0.0001$; paired t-test, GraphPad Prism

C = Significantly different from respective contralateral joint, $p<0.05$; One-way ANOVA, Tukey's post hoc test, GraphPad Prism

S = Significantly different from respective SHAM joint, $p<0.05$; One-way ANOVA, Tukey's post hoc test, GraphPad Prism

AM = Significantly different from respective age-matched joint, $p<0.05$; One-way ANOVA, Tukey's post hoc test, GraphPad Prism

‡ = Baseline (0d) values used for statistical comparison at 3, 7, and 14-days post-DMM

Supplementary Figures:

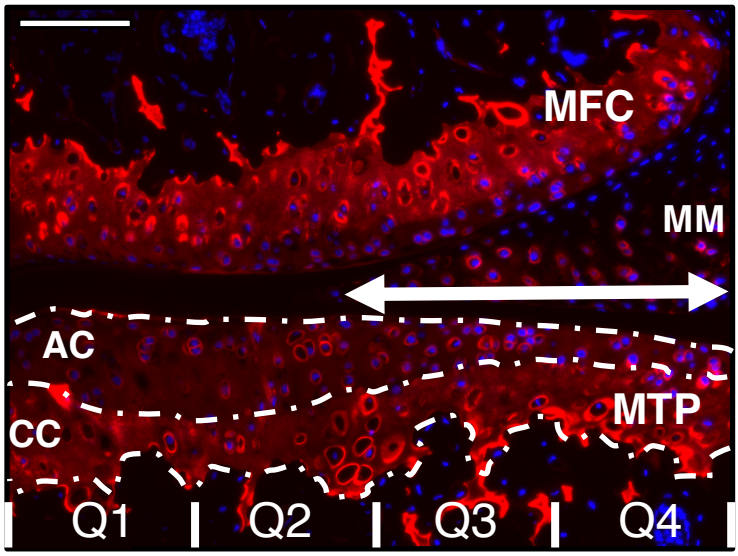

Supplementary Figure 1. Quantification of meniscal coverage, chondrocyte cellularity, and cartilage thickness. Immunohistochemical staining for type II collagen (tissue structural indicator) and DAPI-counterstain (chondrocytes presence) was performed on coronal sections spanning the cartilage-cartilage contact (level 2-4) of the medial compartment of the knee joint. Using a custom MATLAB algorithm, 1) the articular cartilage (AC), calcified cartilage (CC), and medial meniscus (MM) were manually traced; 2) the total number of DAPI-positive cells were counted in the AC and CC; and 3) cartilage thickness and chondrocyte number was quantified for each of four separate regions, quadrants 1 (Q1) through quadrant 4 (Q4), which represent the innermost through outermost regions of the AC, respectively. Furthermore, 4) the degree of meniscal coverage (MM width/AC width) was quantified with respect to the MTP joint margin. Lastly, not shown in the image 5) the extent of linear cartilage damage (including histological values of ≥1) was manually traced in each section. Analysis was restricted to MTP. The AC and CC are outlined in dotted white lines, and the extent of meniscal coverage is indicated via the white arrows. A representative image of a control joint, oriented with the medial joint margin to the right is shown. Scale bar = 100μm.

.

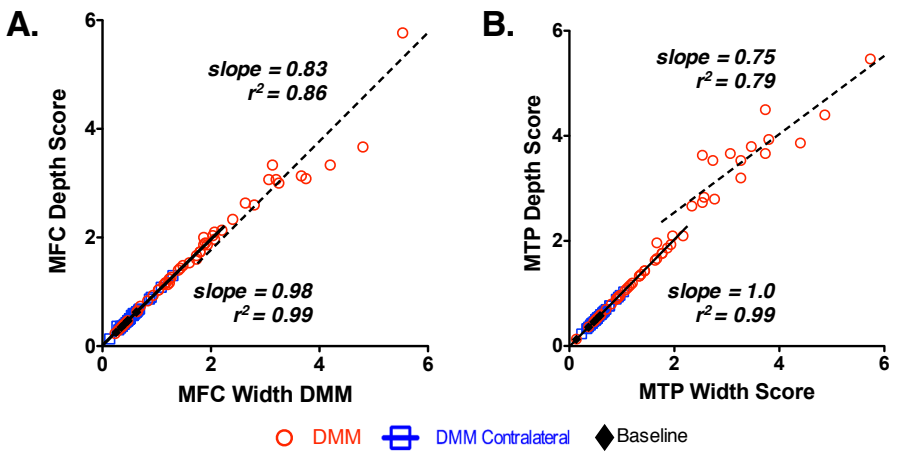

Supplementary Figure 2. Pair-wise comparison of semi-quantitative overall width- vs. depth-wise cartilage damages scoring in the medial joint compartment. To determine if a preference for overall width- vs. depth-wise erosional damage could be observed post-DMM, linear regression was performed on our paired semi-quantitative histological MTP and MFC damage scores. Since damages scores ≤2 are identical in both scoring systems, we observed an expected linear regression slope of ~1.0 for damage scores ≤2 in both the MFC (A.; slope = 0.98) and the MTP (B.; slope = 1.0). However, for damage scores >2 we observed a slight preference towards increased width-wise erosion compared to depth-wise in the MTP (slope = 0.75, p=0.02, extra sum-of-squares F test against a hypothetical slope of 1.0). No preference was observed in the MFC (slope = 0.83, p=0.12). Linear regression r^2- and p-values are shown for values ≤2 and values >2; data for DMM, contralateral and baseline joints are included.

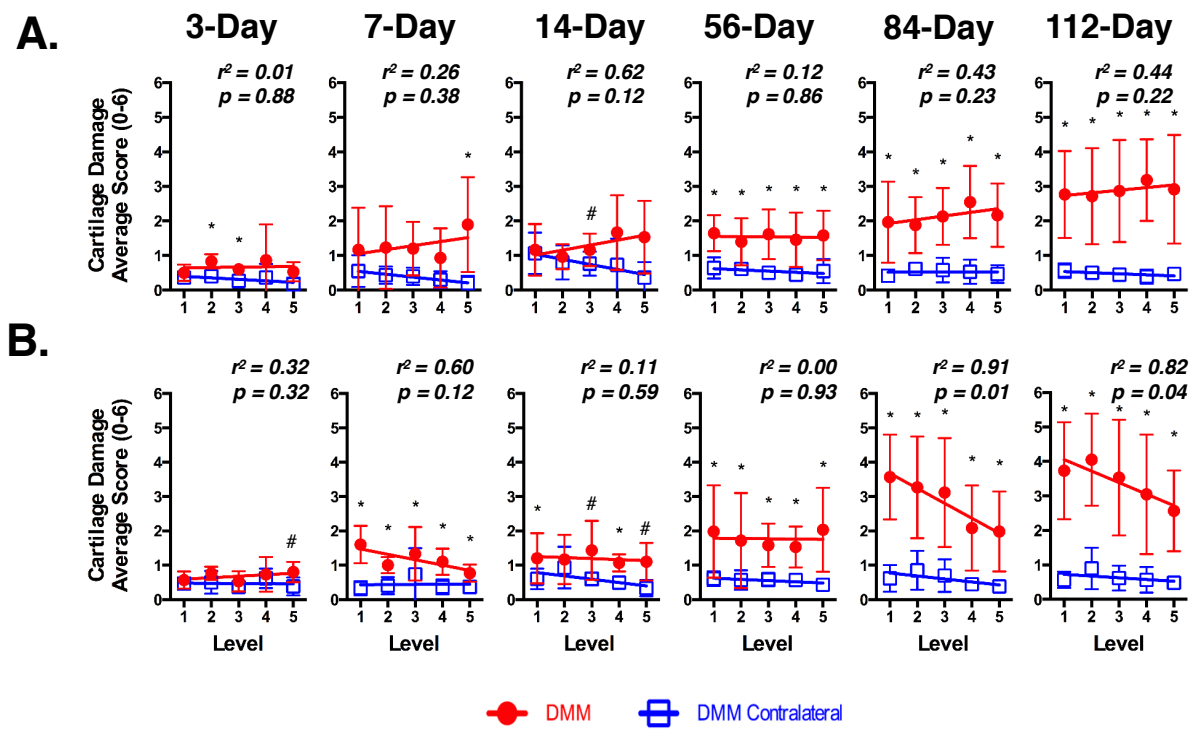

Supplementary Figure 3. Anterior-to-posterior distribution of depth-wise damage within the medial compartment of DMM joints. The distribution of semi-quantitative depth-wise cartilage damage scores in the medial femoral condyle (MFC; A.) and tibial plateau (MTP; B.), from anterior (level 1) to posterior (level 5) aspects of the central cartilage contact of the joint, were evaluated overtime. Similar to the distribution of damage in the width-wise analysis, no preference for localized damage anteriorly or posteriorly was observed in the MFC post-DMM; again, the MTP demonstrated significantly increased damage anteriorly compared to posteriorly at late time-points (84- and 112-days) post-DMM. Results are presented as mean ± STD (n = 5-10/time point/group) where * = $p<0.05$ and # = $p<0.10$ (trend) for paired t-test between DMM and DMM contralateral joints at a given level. Linear regression r^2- and p-values are shown for DMM joints only.

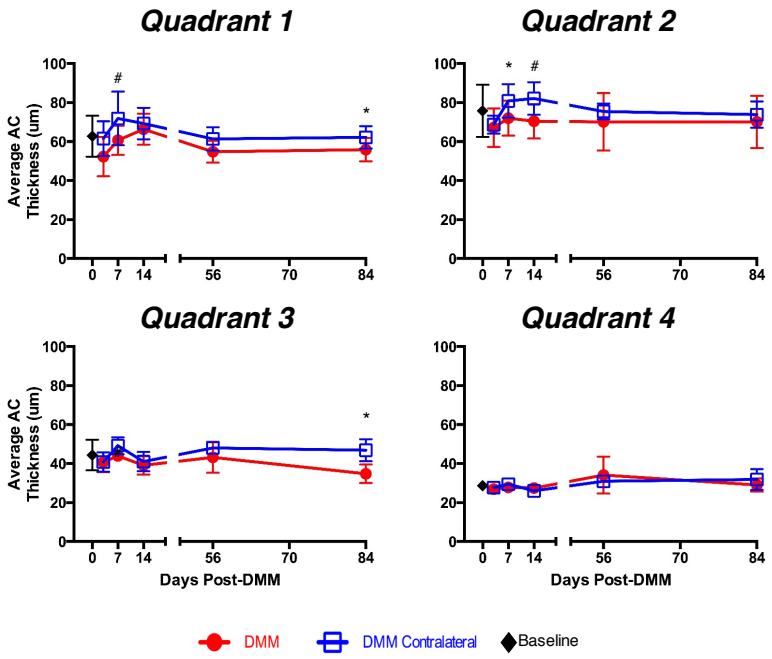

Supplementary Figure 4. Spatiotemporal quantification of articular cartilage thickness across the MTP following DMM-injury. The cartilage thickness of medial tibia plateau (MTP) post-DMM was quantified from manual traces of the AC in collagen-type 2 stained sections. AC thickness measures were obtained, in MATLAB using a Euclidian distance transform, for the four separate quadrants of the MTP. A significant decrease in articular cartilage thickness was only observed within MTP quadrant 3 (Q3) at 84-days. Results are presented as mean ± STD (n = 5/time point/group) where * = $p<0.05$ and # = $p<0.1$ (trend) for paired t-test between DMM and contralateral joints.

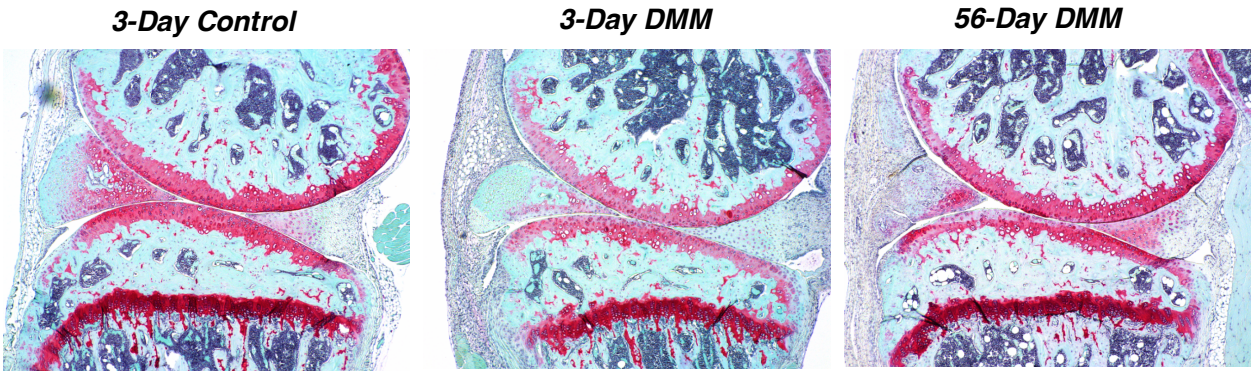

Supplementary Figure 5. Sagittal sections of the anterior-to-posterior distribution of cartilage damage post-DMM. A subset of injured DMM and DMM contralateral joints were sagittally sectioned and stained across the entirety of the joint with Safranin-O/fast green to visual the anterior-to-posterior and medial-to-lateral distribution of cartilage damage at 3- and 56-days post-DMM. Representative images localized to approximately quadrant 3 are shown; the sections are oriented with the femur on top, tibia on the bottom, and the anterior of the joint to the left. At 56-days post-DMM there is clear anteriorly-localized cartilage damage in the medial tibia plateau and to a lesser extent in the medial femoral condyle. No preferential localization of damage was observed at 3-days in either the condyle or tibial plateau. Additionally, in looking across the entirety of the joint at 3-days post-DMM we did not observe the presence of any direct surgical trauma to the articular cartilage following the surgical transection of the MMTL in the DMM procedure.

SB^{3}C2016
Summer Biomechanics, Bioengineering and Biotransport Conference
June 29 –July 2, National Harbor, MD, USA

SPATIO-TEMPORAL QUANTIFICATION OF CARTILAGE STRUCTURAL CHANGES IN A MURINE MODEL OF POST-TRAUMATIC OSTEOARTHRITIS

Michael A. David (1), Avery T. White (1), Rachael Pilachowski (1), Ryan C. Locke (1), Melanie K. Smith (1), Christopher Price (1)

(1) Biomedical Engineering
University of Delaware
Newark, Delaware, United States

INTRODUCTION

Post-traumatic osteoarthritis (PTOA), an accelerated form of OA, results from traumatic joint injury, e.g., ligament and meniscal tears, and is common in active individuals, e.g., athletes and uniformed service members. Approximately 50% of patients that experience a ligamentous tear will exhibit cartilage damage within 10- to 15-years of the injury [1]. Unfortunately, preventative treatments for PTOA are lacking, potentially due to a preclinical focus on mid-to-end-stage disease, whereas the initial changes precipitating PTOA remain largely unknown [2]. In order to develop prophylactic, chondro-protective therapies it is necessary to understand the natural time-course of cartilage structural degradation within the joint during the progression of PTOA. Knowledge of the spatial and temporal progression of cartilage degeneration across the injured joint, heretofore underappreciated, is critical to defining and interpreting the cartilage biology and pathophysiology underlying PTOA, and whether they are of mechanical or cellular origin. Therefore, the objective of the present study was to provide a detailed spatio-temporal histological quantification of cartilage structural changes from early (3-day) through late-stage (112-days) disease in a surgically-induced, murine joint instability model of PTOA, the destabilization of the medial meniscus (DMM) [3]. We hypothesized that cartilage damage would occur early following a traumatic injury and that the cartilage damage would be preferentially localized to the anterior regions of joint where surgical induced joint-instability results in altered biomechanical contact.

METHODS

Animals and Surgeries: Male C57BL/6 mice (Jackson Labs) at the age of 12-weeks underwent DMM surgery in right limbs with contralateral limbs serving as internal controls (n = 5-10mice/group) were harvested at baseline (0d), 3-, 7-, 14-, 28-, 56-, 84- or 112-days post-injury. *Histological Processing:* Samples were immediately fixed (in a naturally flexed position), decalcified, embedded in paraffin, and serially cut into 5-μm thick coronal sections. Starting at the front of the joint (anterior), two-sections were selected approx. every 100-um and stained with Safranin-O/Fast Green to assess changes in cartilage structure. From these, five sets of sections spanning the cartilage-cartilage contact (~500-μm wide) of the tibial plateau and femoral condyle were selected for scoring. *Scoring:* Scoring was performed across all stages of disease development to establish the natural time-course and spatial distribution of cartilage damage following DMM. Three blinded scorers semi-quantitatively ranked cartilage damage in each section using two separate metrics adapted from prior versions of scoring systems [4-6]. First, the extent of cartilage damage across the width of articular surface (referred to as width-based; Figure 1), and second, the extent of depth-wise articular/calcified cartilage damage (referred to as depth-based; Figure 1). For each metric, cartilage damage was assessed on a 0-6 scale for both the medial and lateral femoral condyles and tibial plateaus, and utilized for both temporal and spatial analysis. For temporal analysis, a single average joint score was aggregated for each specimen based upon each scorer's findings, and used to calculate the group mean and SD for each time point. For spatial analysis, an average score at each section location (anterior to posterior) was aggregated from each scorers findings, and used to calculate a spatial location mean and SD for each location and time point. *Statistical Analysis:* To establish differences in cartilage damage between DMM and contralateral joints at each time point, paired t-tests well as one-way ANOVA with post-hoc and linear regression across location were performed. Statistical significance was set at $p<0.05$. Data is presented as mean ± standard deviation

RESULTS

We found significant, site-specific cartilage damage across the medial compartments of DMM joints. No significant damage was observed in the lateral compartments of DMM joints or in any region of the control joints. Temporally, significant cartilage damage appeared as early as 3-days post-injury in the MTP, observed as a loss of proteoglycan staining (Figure 2). Cartilage structural damage in MTP and MFC continued to increase with time under both scoring methods, with the most damage seen at 112-days post-injury. Spatially, we observed trends of cartilage damage that appeared greater in the anterior region of the tibia compared to posterior (Figure 3); however these findings were only significant at 84- and 112-days post-injury. No differences existed at any time point post-injury within the MFC.

DISCUSSION

By combining two scoring methods with temporal and spatial analyses this study provided a detailed representation of the extent and timing of focal vs. widespread cartilage damage, from anterior to posterior, in the joint following injury. We found early and highly localized cartilage damage within the medial compartments of DMM joints. An initial loss of proteoglycan content (3-d), followed by fibrillations/erosion of articular cartilage (7-d), cumulating in full cartilage loss by 112-days post-injury was observed. When compared to the literature, our observation of cartilage damage from 14-days onward post-DMM is entirely consistent with others findings from DMM models in mouse [7-9], rat [10], and rabbit [11]. However, to the best of our knowledge, no group has investigated cartilage damage from 3-7 days post injury in the murine DMM model of PTOA. Our temporal findings suggest that studies attempting to prophylactically prevent PTOA initiation and progression may require immediate-early interventions (≤ 7d in mice) to be most efficacious.

Moreover, we also observed a spatial localization of cartilage damage in the MTP, but not in the MFC. While a trend for increased MTP damage anteriorly was seen at several time points, statistical significance was only found at the later time points (84 and 112-days). These findings support the idea that the insult of the DMM causes altered loading and presumably increased localized contact stress at the front of the joint (anteriorly). There was no difference in damage spatially in the MFC, which suggests that the MTP and MFC may experience different mechanical loading and articulation patterns following DMM. Importantly, our spatial findings are consistent with qualitative observations made in the pioneering murine DMM study where increased damage was found anteriorly [3]. In addition, other animal DMM models have shown spatially localized changes in cartilage damage (medial to lateral) [10] as well as increased medial compartment peak contact stresses [11]. Non-invasive murine models have also shown localization of cartilage damage and chondrocyte apoptosis that is dependent on magnitude and location of force applied [12]. Taken together, these studies and ours suggest that insult and altered loading may be an important factor in rapid precipitating and progressing cartilage damage post-injury.

Qualitative analysis of the localization of cartilage damage has additionally suggested that temporal- and spatial-localization of damage to the MTP cartilage, and its subsequent cellular response (loss of chondrocytes), may be related to changes in meniscal coverage of the articular surface following DMM (Figure 4). We are presently quantifying this relationship, as well as investigating if spatial-temporal changes in other joint tissues, e.g., synovium, bone, and menisci, occur post-DMM.

This study is significant in that it's the first to provide a detailed analysis of the spatio-temporal cartilage changes within the murine DMM model of PTOA from early (3-day) through late (112-day) stage disease. Overall, our findings establish a baseline for the detailed study of the cellular and molecular pathoetiology of PTOA, as well as its prevention through the use of novel, targeted, prophylactic chondro-protective therapeutics.

ACKNOWLEDGEMENTS

This research was funded by DoD PR120788P1. Special thanks to Brianna Gietter and Fiona Flowerhill for their assistance in this project.

REFERENCES

[1] Gillquist, J. et al., *Sports Med*, 27.3, 143-156, 1999; [2] Anderson, D. D. et al., *JOR*, 29.6, 802-809, 2011; [3] Glasson, S.S. et al., *Osteoarthritis Cart*, 15.9, 1061-1069, 2007; [4] Glasson, S.S. et al., *Osteoarthritis Cart*, 18, S17S23, 2010; [5] Chambers, M.G. et al, *Arth Rheum*, 44.6, 1455-1465, 2001; [6] Poulet, B. et al., *Arth Rheum*, 63.1, 137-147, 2011; [7] Kim, B.J. et al., *Tissue Engineering and Regenerative Medicine*, 10.4, 211-217, 2013; [8] Loeser, R.F. et al., *PloS one*, 8.1, e54633, 2013; [9] Gardiner, M. D. et al., *Osteoarthritis Cart*, 23.4, 616-628, 2015; [10] Iijima, H. et al., *Osteoarthritis Cart*, 22.7, 1036-1043, 2014; [11] Arunakul, M. et al., *JOR*, 31.10, 1555-1560, 2013; [12] Wu, P. et al., *Arth Rheum*, 66.5, 1256-1265, 2014.

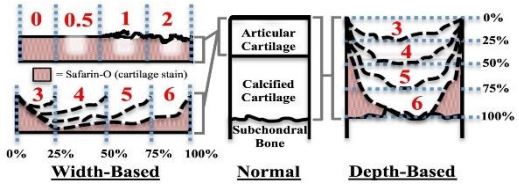

Figure 1: Schematic of width- and depth-based scoring on 0-6 scale (0 normal and 6 being the most cartilage damage). Scoring of 0-2 in both systems are identical. Width is scored irrespective of depth, and vice versa.

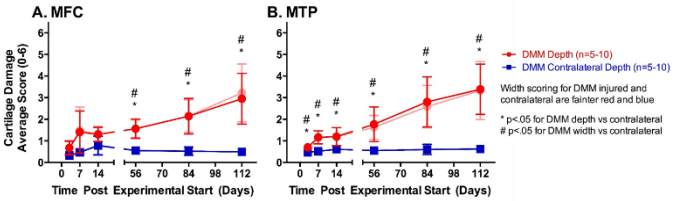

Figure 2: Temporal quantification of cartilage damage width- and depth-wise in the MFC (A) and MTP (B) post-DMM.

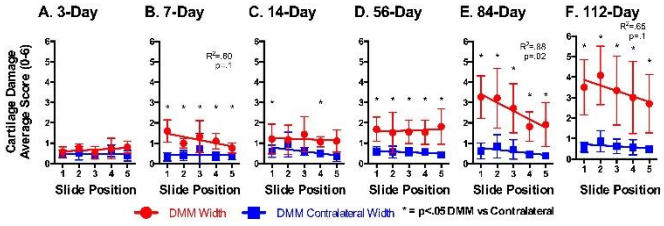

Figure 3: Spatial quantification of cartilage damage, width-wise in MTP post-DMM (A-F) from anterior (position 1) to posterior (position 5) regions of the joint. Regression data only indicated for DMM.

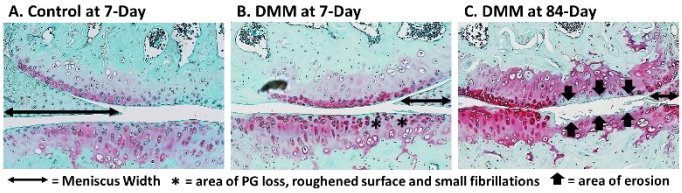

Figure 4: Extrusion of meniscus with medially localized cartilage damage in control (A) & DMM joints at 7- & 84-d (B&C) [position 2 shown].

2015 Biomedical Engineering Society (BMES) Annual Meeting

Title of Abstract: Quantification of Early Structural Joint Changes in a Murine Model of Post-Traumatic Osteoarthritis

Michael A. David[1], Melanie K. Smith[1], Avery T. White[1], Ryan C. Locke[1], Christopher Price[1]
Biomedical Engineering, University of Delaware[1]

Introduction: Post-traumatic osteoarthritis (PTOA), an accelerated form of OA, results from traumatic joint injury, e.g., ligament tears, and is common in active individuals. ~50% of patients experiencing a ligamentous tear will exhibit OA within 15-years [1]. Currently, preventative treatments for PTOA are lacking, potentially due to a preclinical focus on mid-to-end-stage disease, whereas the initial precipitating changes remain largely unknown [2]. Herein, we present a detailed quantification of joint changes from early through late-stage disease in a murine joint instability model of PTOA, the destabilization of the medial meniscus (DMM) [3].

Materials and Methods: Adult mice (12-wk male C57BL/6J) underwent DMM surgery in the right joints with contralateral serving as an internal control. Surgical and control joints were harvested at baseline (0-), or 3-, 7-, 14-, 28-, 56-, 84- and 112-days post-injury. Samples were immediately fixed, decalcified, embedded in paraffin, and cut to 5-μm thick coronal sections. To assess PTOA-induced structural damage, mid-joint sections were stained with Safranin-O/Fast Green. Three blinded individuals scored the extent of cartilage damage on tibial plateau and femoral condylar cartilage using a modified, semi-quantitative scoring system, as well as the degree of synovitis and osteophyte formation (medial compartments only) [4,5]. Paired t-tests (significance set at $p<0.05$) were performed at each time point between DMM joints and contralateral joints.

Results and Discussion: We found significant site-specific cartilage damage in the medial compartments of DMM joints that appeared as early as 7-days post-injury and increased with time (Figure 1A). No significant cartilage damage was observed in the control joints. Furthermore, the development of synovitis (Figure 1B) and osteophyte formation (Figure1C) appeared as early as 3-days post-injury in the medial compartments of DMM joints. These results suggest that structural changes in the joint, including bone, cartilage, and synovium responses, are initiated earlier than previously appreciated. Thus, studies attempting to prophylactically prevent PTOA initiation and progression may require immediate-early interventions (≤ 7d in mice) to be most efficacious.

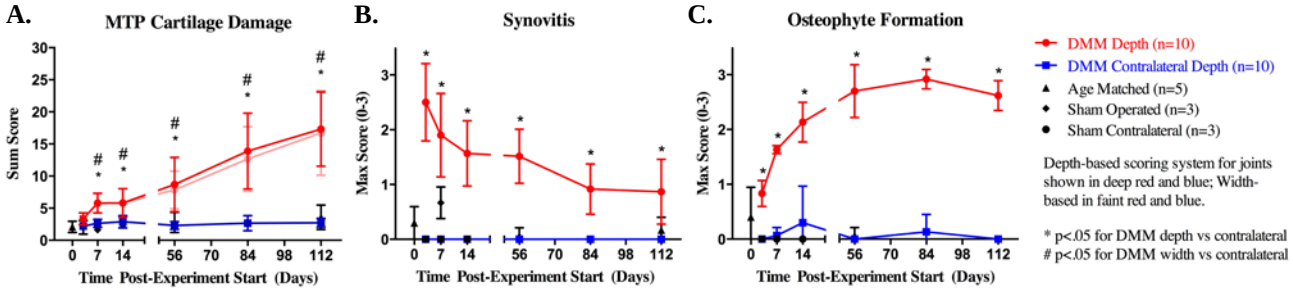

Figure 1. Semi-quantitative scoring of structural changes in the medial compartments of DMM and control joints. Scoring of (A) medial tibia plateau (MTP) cartilage damage, (B) synovitis, and (C) osteophyte formation. Results are represented as mean ± SD.

Conclusions: Overall, the results of this study demonstrate evidence of significant early (by 7-day) structural changes in the murine DMM model of PTOA, and establish a baseline for the detalied study of the cellular and molecular pathoetiology of PTOA and its prevention through the use of novel, targeted, prophylactic chondroprotective therapeutics.

Acknowledgements: This research was funded by DoD PR120788P1. Special thanks to Brianna Gietter and Fiona Flowerhill for their assistance in this project.

References: [1] Gillquist, J., Sports Med, 1999, 27.3, 143-156; [2] Anderson, D. D., JOR, 2011, 29.6, 802-809 [3] Glasson, S.S., Osteoarthritis Cart, 2007, 15.9,1061-1069; [4] Glasson, S.S., Osteoarthritis Cart, 2010, 18, S17-S23; [5] Chambers, M.G., Arth Rheum, 2001, 44.6, 1455-1465.

2015 Biomedical Engineering Society (BMES) Annual Meeting

Depth- vs. Width-Wise Quantification of Cartilage Damage Following Joint Destabilizing Surgery in the Mouse

White, Avery T., David, Michael A., Smith, Melanie K., Locke, Ryan T., Pilachowski, Rachael, Price, Christopher
Department of Biomedical Engineering, University of Delaware, Newark, DE

Introduction: Post-traumatic Osteoarthritis (PTOA) is the rapid degeneration of the articular cartilage that often follows serious joint injury, *e.g.*, ruptured ligament or torn menisci. Historically, two semi-quantitative scoring systems (width- or depth-based) have been utilized for ranking the extent of cartilage damage in various animal models of PTOA[3,5]. Although both methods provide useful information on the etiology of PTOA, these methods have never been used in combination. Therefore, to fully characterize when and how cartilage damage occurs, we utilized and compared both of these scoring systems from early through late stage disease progression in a murine model of PTOA, the destabilization of medical meniscus (DMM). We hypothesized that combining both scoring systems would provide a more complete understanding of how articular cartilage damage proceeds, either widespread or focally, following joint injury.

Methods: DMM surgery was performed on the right knee of 12-week-old male C57BL/6J mice[4]; contralateral joints served as controls. Joints were harvested 0, 3, 7, 14, 56, 84, and 112-days post-surgery. Upon harvest, joints were fixed, decalcified, embedded in paraffin, and sectioned into 5-µm coronal slices. PTOA-related cartilage damage was assessed by staining 5 equally spaced sections surrounding the region of cartilage-cartilage contact (~500-um wide) with Safranin-O/Fast Green. Three blinded individuals scored, using a 0-6 scale, the width- and depth-wise (Figure 1A) extent of cartilage damage in 4 quadrants of the joints: the medial femoral condyle (MFC), lateral femoral condyle (LFC), medial tibial plateau (MTP), and lateral tibial plateau (LTP)[3,5]. Values were averaged across scorers, and a pair-wise calculation of the ratios of each joints' depth vs. width score were calculated for joints with scores > 2. One sample student t-tests (significance set at $p<0.05$) were used to compare the ratios for each compartment to a value of 1, which signifies no preference for depth or width-wise damage.

Results: We found previously that cartilage damage increased in a time-dependent manner from early (3-7- days) to late (86-112-days) stage PTOA only in the medial compartments of the DMM joints (Figure 1B)[6]. Reanalyzing this data, at early time points differences among scoring systems are not present (values < 2 are equivalent). However, when comparing the ratio of individual DMM joints' depth and width scores greater than 2, the MTP ratios were significantly greater than 1 indicating a preference toward focal, as opposed to widespread, cartilage damage in the MTP (Figure 1C).

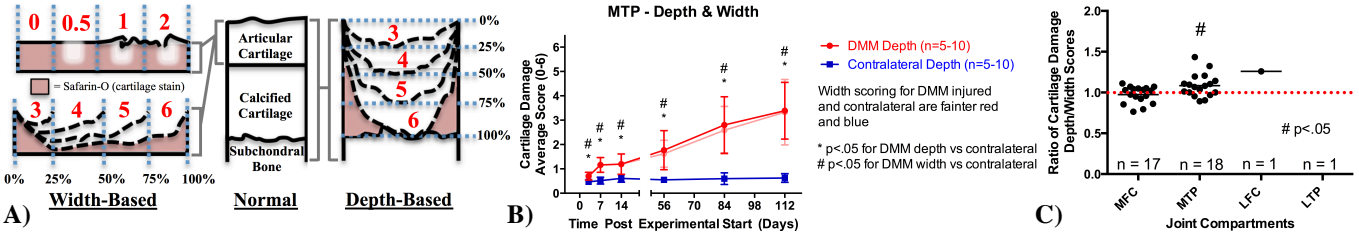

Figure 1: A) Combined scoring system **B)** Time vs. cartilage damage (MTP) **C)** Depth vs. width damage (four quadrants)

Discussion: While the two different scoring methods are informative on their own, implementing them together within our modified scoring system allowed for a more holistic view of the natural progression of focal versus widespread cartilage destruction in the DMM model of PTOA. Specifically, we found a slight, but significant preference for depth-based damage in the MTP but not the MFC of DMM joints (Figure 1C). This concentrated focal cartilage damage could be the result of mechanical or biological processes that occur preferentially at the medial tibial plateau in response to the induced injury.

Significance: Findings from our combined quantification technique can be utilized to visualize tissue level processes involved in the development/progression of PTOA; these will be followed up by extensive immunohistochemical analysis to study the underlying cellular correlates to these processes. These same procedures will also be repeated in studies utilizing novel therapeutic strategies for preventing PTOA after DMM surgery/knee injury. Furthermore, the expansion of the scoring methods described here could be of benefit to other research groups performing similar structural analyses of cartilage.

References: 1.Gillquist, J., *Sports Med* (1999). 2.Maletius, W., *Am J Sports Med* (1999). 3. Glasson, S.S., *Osteoarthr Cartil* (2010). 4. Glasson, S. S., *Osteoarthr Cartil* (2007). 5. Chambers, M.G., *Arth Rheum* (2001). 6. David, M., *ORS Conference* 2015

Center for Biomechanical Engineering Research
Celebrates National Biomechanics Day
Conference Date: April 7, 2016 Deadline: Wednesday, March 9, 2016

Destabilization of the Medial Meniscus in Mice Induces Early, Localized Chondrocyte Loss and Cartilage Damage

Michael A. David[1], Melanie K. Smith[1], Rachael N. Pilachowski[1], Avery T. White[1], Ryan C. Locke[1], Christopher Price[1]
Biomedical Engineering[1], University of Delaware

Post-traumatic osteoarthritis (PTOA) is an accelerated form of osteoarthritic cartilage degeneration resulting from acute joint injury. Approximately 50% of patients experiencing joint injury will exhibit cartilage degeneration within 10-15 years post-injury. Currently PTOA is incurable; to better understand the etiology of PTOA and to develop rational anti-osteoarthritic therapies, it is critical to understand the spatiotemporal initiation and the progression of PTOA from early- through late-stage disease. In this study we employed semi-quantitative damage scoring and quantitative histological analysis of disease progression in the murine destabilization of the medial meniscus (DMM) model of PTOA from early (3-days) through late (112-days) timepoints post-injury. We observed significant, progressive articular cartilage changes in the medial compartments of injured joints as early as 3-days post-DMM. Damage was found to preferentially localize towards the anterior regions of the joint, and furthermore, a near complete loss of chondrocytes (3-days post-DMM), surface damage (7-days), and cartilage erosion (56-days) was found to co-localize to a small region of the medial tibial plateau subjected to post-DMM meniscal uncovering. Taken together, these results suggest that DMM-mediated extrusion of the medial meniscus alters the mechanical environment of the medial joint, leading to rapid, spatially-dependent changes in articular cartilage cellularity and structure, and precipitates the focal degeneration of cartilage associated with PTOA. Importantly, this study suggests that even ‘subtle’ mechanical insults may trigger immediate (<7 days) biological processes that initiate PTOA, and that development of chondroprotective strategies for preventing and/or delaying PTOA-related cartilage degeneration are best targeted toward immediately-early processes following joint injury.